BSc Thesis

Coil Placement in a DIPT System

J. Diender
S. de Jong

Optimizing coil placement in a dynamic wireless charging system in order to reduce voltage fluctuations.

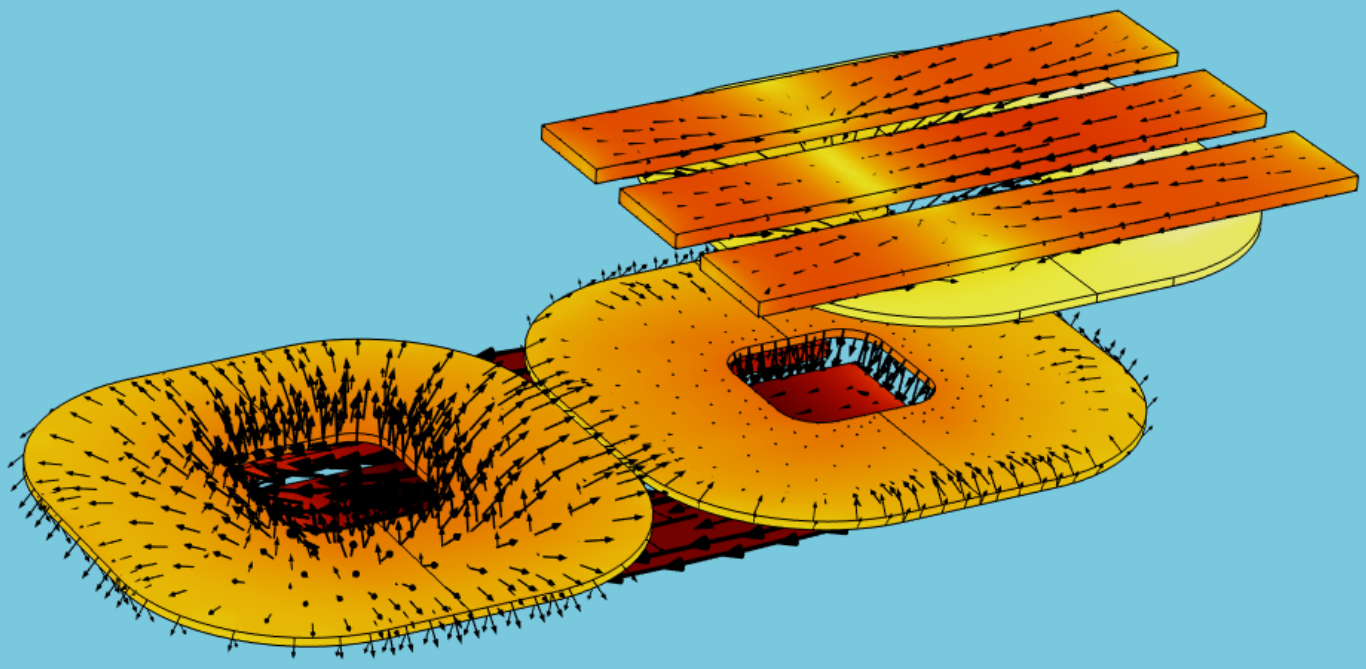

TU Delft

BSc Thesis

Coil Placement in a DIPT System

by

J. Diender
S. de Jong

To obtain the degree of Bachelor of Science
at the Delft University of Technology,
to be defended on Tuesday June 24, 2025 at 11:00 AM.

Student numbers: 5272882 & 5114225
Project duration: 14 April, 2025 – 27 June, 2025
Thesis committee:

Gerard Janssen,	TU Delft, chair
Wenli Shi,	TU Delft, supervisor
Dennis van der Born,	TU Delft

TU Delft

Abstract

The goal of this bachelor thesis is to reduce the voltage fluctuations in a dynamic inductive power transfer (DIPT) system, by determining the optimal coil location and/or spacing. In a segmented DIPT system the output voltage changes as the receiver (Rx) side moves over the transmit (Tx) side. By analyzing the spacings between the Tx- and Rx-coils it is possible to influence the output voltage and its fluctuations. The system studied consists of two rectangular Rx-coils in series, and multiple bipolar Tx-coils.

This research starts by building a model in COMSOL with one Tx- and one Rx-coil. Then a MATLAB program is presented which can simulate the whole system by, among others, phase shifting the original COMSOL data. Finally, the optimal coil location can be determined by comparing the average output voltage and the fluctuation in output voltage for different Tx- and Rx-coil spacings. Different tests are performed to confirm the results of the COMSOL model and the MATLAB simulations. The research showed that this system can not effectively reduce the voltage fluctuations, therefore a parallel configuration of Rx-coils is proposed. Simulation results show that this alternative solution can reduce the voltage fluctuations.

Preface

The following thesis was written as a bachelor graduation project for the BSc Electrical Engineering at the TU Delft. The goal of the project is to find the optimal coil placement in a dynamic inductive transfer system. The final results could help the implementation of DIPT systems for electric vehicles, which will help increase their driving range whilst decreasing the size of their battery.

The project was commissioned and supervised by dr.ir. Wenli Shi. To whom we would like to express our gratitude for his guidance, patience, and advice during this project. We also want to thank Bart Roodenburg for his help during the testing phase. Next to that, special praise goes out to our peer students from the other sub-groups included in this project; Nathan van Himbergen, Stefan Kort, Owen Wattenberg and Jesse Treurniet.

J. Diender
S. de Jong
Delft, Q4 2024/2025

Contents

1 Introduction

People have always had a desire to travel: nomadic tribes, pilgrimage, and oversees travels to discover the world. In the beginning this was done by horse, then by ship, train, and finally with commercial vehicles. The world has changed since then, the effects of carbon emissions are in full view: worsening health, extreme weather and a negative effect on the environment. To reduce emissions, fossil fuel is being swapped with electricity as a main source of power. More and more vehicles are being made electric instead of fossil-fueled. There is a problem that remains. Electric vehicles (EV) provide less traveling freedom then combustion engines.

In 2025, the rise of EVs is clearly visible, a quarter of the new cars being sold worldwide is electric [13]. This might be due to many governments that are encouraging the development of the EV market to reduce greenhouse gasses. Nevertheless, there are a few drawbacks compared to combustion engines: they are more expensive, heavier and take a long time to recharge [15, 17, 18]. There are several solutions that are being investigated such as: improving batteries, battery swapping stations and dynamic wireless charging of EVs [15].

A lot of research is being done on how to make batteries more efficient. The research into batteries is already quite mature [28], but a lightweight, power-efficient battery which is in direct competition with fossil fueled car has yet to be found. A second option would be a battery swapping station, however new limitations arise with this solution, batteries need to be interchangeable, the cost for a second battery is quite high and there are safety concerns with storing large amounts of batteries [14]. A different way to extend the driving range is by using a dynamic inductive power transfer system, enabling EVs to be charged while driving [4, 7, 20]. This allows the driving range to be extended while keeping the battery compact.

The ideal situation is a reliable, efficient and cost effective charging method to allow EVs to be the transportation method of the future.

1.1. System description

Such a DIPT system can be divided into three parts, as illustration is depicted in Fig. 1.1. Each part of the system is being researched by a different subgroup as part of the TU Delft Electrical Engineering Bachelor's End Project.

The first part is the controller [10]. Using feedback- or feedforward control, this controller ensures that the system delivers a smooth supply of power to the EV, by generating a reference voltage signal for the PWM controller of the inverter.

The inverter combined with the PWM controller and the rectifier constitutes the second part of the system, the converter [24]. This part of the system converts a DC input voltage to an AC voltage for the coils on the transmitter (Tx) side, and rectifies the AC voltage to a DC voltage on the receiver (Rx) side.

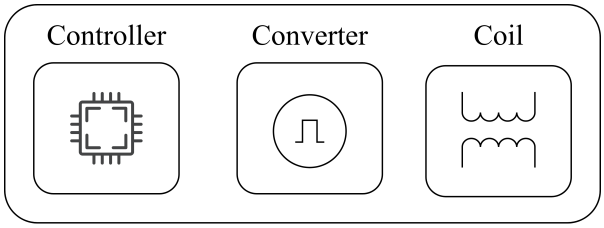

Figure 1.1: Overview of the three parts, and subgroups, for the proposed DIPT system

The last part of the system is the magnetic coils, which allow the system to wirelessly transfer power from the Tx- to the Rx-coil. In a dynamic inductive power transfer (DIPT) system, the Tx-coils are embedded in the road, and transfer power to the Rx-coils, which are in a moving object. This thesis focuses on the coil part of the DIPT system.

1.2. Document scope, bounding and structure

The success of the proposed system depends on it being cost effective, power efficient, and reliable, the SMART criteria will be discussed in length in Chapter 2. This thesis will explore a segmented DIPT system, allowing the coils to be kept relatively small, which will make it more cost effective. Additionally, there are less coils needed because there will be a strategic amount of spacing between the Tx-coils. To meet the set goals, it is crucial to keep the power transfer fluctuations within certain bounds. This prevents a costly and over designed Rx-side converter.

In a DIPT system, the power is transferred through the mutual inductance between the Tx-coils, and a moving Rx-coil. The movement of the Rx-coil causes fluctuations in the mutual inductance [5, 9, 31]. As the mutual inductance is directly related to the power that is transferred, this also results in power fluctuations. To reduce the fluctuations in the mutual inductance this thesis will look at a crucial factor: the relative coil locations [4, 15, 18, 22]. Finding the optimal coil spacing between the Tx-coils will help minimize the fluctuations. Additionally, a second Rx-coil will be added to further optimize the system. That results into two spacing parameters that can be changed in the scope of this thesis: the spacing between the transmit coils and the spacing between the receive coils.

The system is limited by a number of constraints. Firstly, the receiver is mounted on the EV, meaning the available space and weight are limited. Therefore, components on the receiver side should be selected with that in mind. Furthermore, the magnetic coupling between the Tx- and Rx-coils is limited by an air-gap of 5 cm. To achieve the rated power the output current needs to be rather high. As compensation for the low magnetic coupling, the winding currents tend to be relatively high to reach the rated power. Which in turn, will cause conduction losses, making the efficiency of the power transfer limited. To improve the efficiency a compensation circuit will be added.

Lastly, there is the problem of misalignment. If the system is implemented to charge EV whilst driving, there will be misalignment between the Tx- and Rx-coils which needs to be accounted for. It can be concluded that there are four variables to monitor the performance of the system: power transfer efficiency, misalignment tolerance, mutual inductance, and transferred power fluctuations.

The problem can thus be narrowed down to the following question that forms the base of this thesis: **How to minimize fluctuations in the mutual inductance of DIPT system, by optimizing the relative Tx- and Rx-coil locations and/or spacings?**

This thesis will first explore the fundamental physical principles behind the mutual inductance mechanism in Chapter 3. After this, two different coil topologies, and two different compensation circuits for DIPT systems will be discussed in Chapter 4. Followed Chapter 5, explaining the modeling of the system of coils, and its simulated results. Using the obtained simulated data, Chapter 6 describes the how the optimization of the coil spacings can be used to minimize mutual inductance fluctuations. Next, Chapter 7 discusses the testing and verification performed on the system. An alternative system, called the double Rx side, is proposed in Chapter 8. Followed by a discussion on hurdles, and improvements found during the thesis. Finally, the results and the conclusion are summarized in Chapter 10.

2

Program of requirements

The following chapter will discuss requirements of this thesis which serve as a starting point for the upcoming chapters. To ensure that the performance requirements are evaluable they will be held up against the so called SMART-criteria. Hance, every requirement should be specific, measurable, assignable, realistic and time-related. First, the global project requirements, shared with the other sub-groups, will be discussed. Second, the requirements specific to this thesis are presented.

2.1. Global system requirements

The global system requirements are shared between all three sub-groups of this BSc thesis project. They consist of number of functional requirements, followed by specific performance requirements.

2.1.1. Functional requirements

A.1 The Tx- and Rx-side of the system must be separated without a physical link.

A.2 The complete system must be able to inductively transfer power to a moving vehicle (dynamic).

A.3 The complete system must be able to lower the amount of power ripple, compared to a non-controlled standard situation.

A.4 The system must operate on the specified, already established hardware in the ESP lab.

A.5 The system must be physically tested during the project scope.

A.6 The radiated power must not be harmful for humans.

2.1.2. Performance requirements

B.1 The system operates on a switching frequency of 85 kHz.

B.2 The system has a maximum input voltage of 100 V.

B.3 The system has a maximum input current of 10 A.

B.4 The system must be able to invert the voltage from a DC power supply.

B.5 The system must be able to rectify the outgoing current on the receiver side.

2.2. Coil-group requirements

The requirements set in this section are solely applicable to this thesis, and thus form the most important criteria this thesis is developed on. They again consist of number of functional requirements, followed by specific system requirements.

2.2.1. Functionality requirements

1.1 The system of coils must be able to transfer power in a dynamic matter; in this situation the Tx-coils are static and the Rx-coils will move.

1.2 A COMSOL model of the working principles, which entails modeling the electromagnetic field for the system of coils, must be made.

1.3 The resulting COMSOL data must agree to an explainable level with the real tested data, such that it is deemed accurate.

1.4 A functioning MATLAB program, extending the COMSOL model to a multiple coil system must be written.

1.5 The MATLAB program should be easily extendable to a set number of Tx- and Rx-coils.

1.6 Testing on the already available system of coils must be performed.

1.7 Both the COMSOL and MATLAB data must be compared with the obtained test-data.

2.2.2. System requirements

Performance requirements

2.1 The maximum V_{out} ripple in the system must not be higher then 20 %.

2.2 The mutual inductance between the Rx- and respective Tx-side must never be 0 H.

2.3 The fluctuation in mutual inductance between the Rx- and respective Tx-side must never exceed 20 %.

2.4 The vertical distance, in the z-axis, between the Tx- and Rx-coils is 5 cm.

2.5 The horizontal distance, in the x-axis, between adjacent Tx-coils must never exceed 14 cm.

2.6 On the x-axis, the adjacent Tx-coils must never overlap.

Modeling and simulation requirements

3.1 The simulations of the systems of coils must be reproducible using *COMSOL Multiphysics 6.2* and *MATLAB R2024b*.

3.2 The simulations done must not deviate more than 10 % from the results obtained from same circumstances real-world tests.

3

Coupled coils

Inductive Power Transfer (IPT) is a method of wireless energy transmission that uses electromagnetic fields to transfer power between two or more coils. The fundamental operation of an IPT system relies on the mutual inductance between a transmitting (Tx) coil on the primary side, and a receiving (Rx) coil on the secondary side. When obtaining resonance at both sides, high efficiency, and transmitted power can be achieved. This chapter will discuss and explore the physics behind IPT systems used later on in this thesis.

3.1. Coil physics

The self-inductance of a coil is defined by the magnetic flux captured by the surface of the coil, the number of turns, and the current going through the coil, as depicted in Eq. 3.1.

$$L_{\text{self}} = \frac{N\phi_{\text{coil}}}{I_{\text{coil}}} \tag{3.1}$$

Fig. 3.1 shows a relationship between the magnetic flux's, coil currents, and the coil voltage in case of two coils. Notice that the current going through one coil induces a magnetic flux in itself, as well as in the other coil.

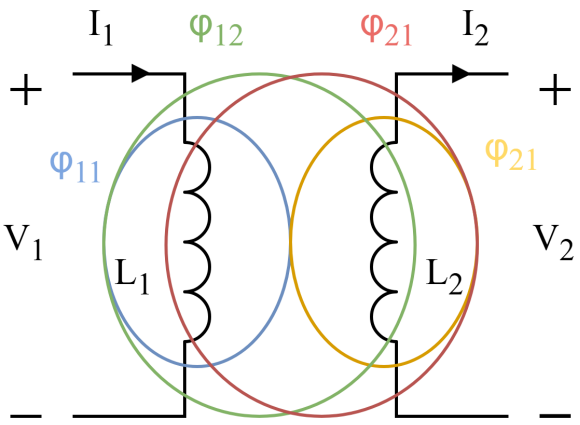

Figure 3.1: Currents and the resulting magnetic flux for coupled coils

Therefore Eq. 3.1 changes to Eq. 3.2, including the mutual fluxes resulting from the other coil(s).

$$L_1 = \frac{N_1(\phi_{11} + \phi_{12})}{I_1} \tag{3.2a}$$

$$L_2 = \frac{N_2(\phi_{22} + \phi_{21})}{I_2} \tag{3.2b}$$

Using Faraday's law, both coil voltages in Fig. 3.1 can be determined as described in Eq. 3.3.

$$V_1 = N_1 \frac{d(\phi_{11} + \phi_{12} - \phi_{21})}{dt}, \tag{3.3a}$$

$$V_2 = N_2 \frac{d(\phi_{22} + \phi_{21} - \phi_{12})}{dt} \tag{3.3b}$$

The mutual magnetic flux components, ϕ_{12} and ϕ_{21}, allows energy, and thus power, to be transferred from one side to another. Whereas the magnetic flux components, ϕ_{11} and ϕ_{22}, are defined as the leakage magnetic flux. The energy balance in this interaction is defined as the mutual inductance (M), which is given by Eq. 3.4.

$$M = N_1 i_1 \frac{\phi_{21}}{dt} = N_2 i_2 \frac{\phi_{12}}{dt} \Rightarrow \frac{N_1 \phi_{21}}{i_2} = \frac{N_2 \phi_{12}}{i_1} \tag{3.4}$$

The transferred power has two parts, active (P) and reactive (Q). Active power is consumed in the circuit, while reactive power is used to transfer the power into an electric or magnetic field [11, 23]. The reactive power is therefore the power of interest. For a simple coupled circuit as shown in Fig. 3.1, the transferred power can be expressed as in Eq. 3.5.

$$P_{12} = \Re\{j\omega_s M I_{\text{Tx}} I_{\text{Rx}} sin(\phi_{12})\} \tag{3.5}$$

Normally the Tx- and Rx-coils of an IPT system are not physically connected. However, in order to find the mutual inductance, testing is performed using an LCR-meter, for which all the coils in the system need to be connected in series. This is possible in two ways, either series aiding or series opposing. If the coils are connected in series aiding the total inductance is as described in Eq. 3.6.

$$L_{\text{total}} = L_1 + L_2 + 2M \tag{3.6}$$

If the coils are connected in series opposing, the total inductance is as described in Eq. 3.7.

$$L_{\text{total}} = L_1 + L_2 - 2M \tag{3.7}$$

3.2. Quasi-static modeling

The physical mechanism behind two coupled coils stems from the Maxwell-Faraday equation shown in Eq. 3.8. The equation shows that there are two ways a magnetic field can be induced, either by varying the electric field in the time- or space domain. An DIPT system has both a time and spatially varying electric field.

$$\Delta \times E = -\frac{dB}{dt} \tag{3.8}$$

For two coupled coils, the magnetic flux induced by the current in the first coil is equal to the magnetic field going through surface of the second coil [23, 25]. Eq. 3.9 describes this relation.

$$\phi_{\text{coil}} = \int_S B \cdot ds \tag{3.9}$$

When the alternating current (AC) of a stationary coupled coil system flows through the primary coil, it generates a time-varying magnetic field that induces an electromotive force (EMF) in the secondary coil, described in Eq. 3.10.

$$V_{\text{EMF}}^{tr} = -N \int_S \frac{dB}{dt} \cdot ds \tag{3.10}$$

A second EMF is induced by the moving Rx-coil with respect to the Tx-coil(s). This motion-dependent EMF voltage is determined by Ampere's law. For a velocity $\mathbf{u}$, with which the coils move respectively from each other, this EMF voltage can be determined by Eq. 3.11.

$$V_{EMF}^{m} = \oint_C (\mathbf{u} \times \mathbf{B}) \cdot d\mathbf{l} \tag{3.11}$$

The total induced EMF on the receiving side is the sum of the time-dependent and motion-dependent EMF. This can be given by the general expression of Faraday's law of induction, Eq. 3.12.

$$V_{EMF} = -N \frac{d\phi_{coil}}{dt} \tag{3.12}$$

However, the operating (switching) frequency and relative velocity determine if both parts are equally present or if the system can be seen as quasi-static. When the latter is true, only the time-dependent EMF has to be accounted for. For the system discussed in this thesis, the specifications are a maximum relative velocity of 0.5 m/s and a switching frequency of 85 kHz, as is the SAE J2954 standard. As the velocity is very small compared to the switching frequency, the effect of the motion-dependent EMF voltage can be neglected as can be seen in Eq. 3.13 [5].

$$v_{motion} \ll f_{switching} \tag{3.13}$$

4

Dynamic wireless power transfer (DIPT) systems

The system discussed in this thesis is designed for dynamic inductive power transfer, meaning that one or more parts are moving in a dynamic manner with respect to each other. A DIPT system has two main components: the transmit (Tx) and the receive (Rx) coil. The design is focused on a segmented DIPT system, hence, multiple Tx-coils are used. To make the system more cost effective the system will be optimized to use the least amount of Tx-coils necessary, while still being able to transfer a minimally fluctuating amount of power. This optimization needs to take into account that the implemented coil design should be compact and light. Moreover, it is important that the system also has an acceptable tolerance to the misalignment [4, 8, 20]. A few strategies are already employed in the physical system used in this thesis to aide this objective.

4.1. Coil topology

A way to influence the power fluctuations in a DIPT system, is the selection of the coil topology. A lot of research on DIPT systems is already being done for elongated coils, for example the Korea Advanced Institute of Science and Technology (KAIST) is looking into powering a bus in motion with such a system [6, 16, 21]. As the leakage inductance is higher, the power efficiency is lower, and the construction cost is high [20, 27]. Therefore, elongated coils will not be discussed in this thesis due to their disadvantages. Instead, the coil topologies discussed are: circular, rectangular, elongated and bipolar.

Bipolar-, or DD-coils are a form of polarized coils, whereas circular and rectangular coils are non-polarized coils. The difference between polarized and non-polarized coils is the path of the magnetic flux. The magnetic flux path of the different coils is illustrated in Fig. 4.1. The non-polarized coils, circular and rectangular, have one magnetic pole. The flux lines exit from this pole and wrap around the outside. A polarized coil has two magnetic poles, Fig 4.1 shows the flux lines coming out of the left half of the coil, wrapping around the outside. The lines connected to the right half then enter the center of the right half and wrap around the outside from the other side [3, 8].

The magnetic flux lines are more dense in the center of a coil and less dense on the outer edges. The change in magnetic flux is related to the magnetic coupling between two coils, when the coil moves over a part where the flux density is high the magnetic coupling is also high. The flux density becomes lower the further away it is from the center of the coil. Consequently, the magnetic coupling is near zero if they are misaligned, as the coil is is the furthest away from the center. As one coil is moved over the other coil, the magnetic coupling will increase as they start to overlap, and will reach a peak when the are perfectly aligned, then decrease again when they have passed each other.

For a polarized coil, there are two areas where the magnetic flux density is highest, since there are two magnetic poles. If a non-polarized coil moves over a polarized coil, the magnetic coupling will start

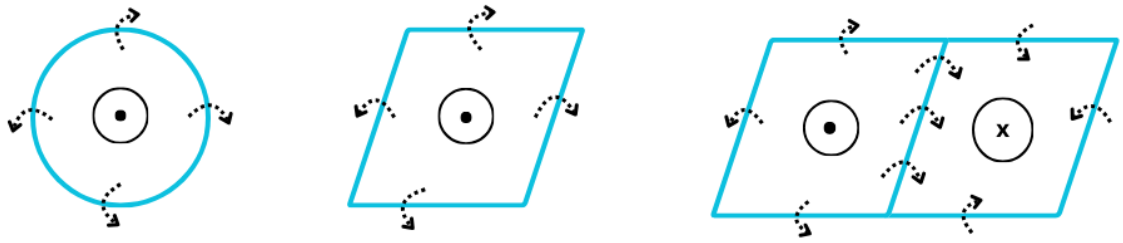

Figure 4.1: The magnetic flux path in a circular, rectangular, and bipolar coil, depicted from left to right

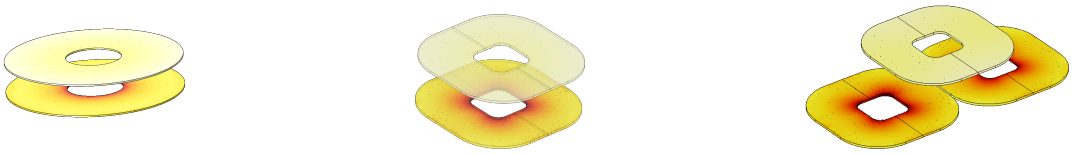

(a) Circular coils (b) Rectangular coils (c) Rectangular and bipolar coil

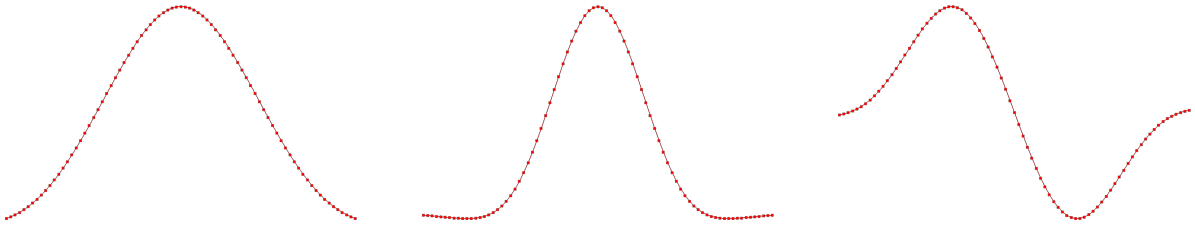

(d) Circular coils (e) Rectangular coils (f) Rectangular and bipolar coil

Figure 4.2: Different coil types (first row) and their mutual inductance curves (second row)

at near zero, then increase as the left half of the polarized and the center of the non-polarized coil align. When the non-polarized coil moves to the center of the polarized coil the magnetic coupling will become zero. As it moves further along the x-axis, the coupling will become negative, with a minimum when the two poles are overlapped. When they are no longer overlapping the coupling will near zero again. Depending on the configuration of the polarized and non-polarized coil the curve can also first become negative and then positive.

The efficiency for the different coil topologies has been widely researched. Overall circular coils are proven to have a higher efficiency than rectangular coil when the are aligned, whilst rectangular coils have a higher misalignment tolerance [12]. Both circular and rectangular coils outperform the DD (polarized) coils during perfect alignment conditions [3]. However, [8] found that bipolar coils have a higher tolerance for misalignment. As the coils are moving with respect to each-other, a circular coil will have more inductance leakage, which lowers efficiency. Therefore, a rectangular or bipolar coil is preferable.

For this thesis a bipolar coil was chosen as a Tx-coil, and a rectangular coil for the Rx-coil. The chosen coils are depicted in Fig 4.3, their specifications are listed in Chapter 5, Table 5.1. The choice for the combination of a bipolar and a rectangular coil was impart due to the higher misalignment tolerance. Moreover, it opens the door to a second receiver coil, which could significantly reduce the fluctuation in output voltage.

The coils are made from so called *"litz wire"*, consisting of approximately 2200 strands, and a diameter of 71 μm. This fine strand diameter is used to minimize high-frequency effects such as skin and proximity losses [20, 4]. These are wound in a rectangular shape, which are visualized in Fig. 5.1. To enhance

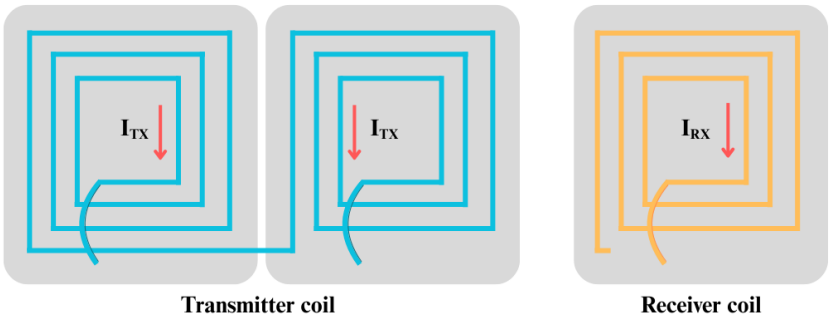

Figure 4.3: Visual representation of the chosen Tx- and Rx-coils

the (mutual) inductance, ferrite can be added to the outside of both the Tx- and Rx-coils. For this, a choice needs to be made between a single sided versus a double sided inductive coupler. A double sided coupler has the coil windings around the ferrite, whereas the single sided coupled uses a ferrite backing. While a double sided coupler can be made smaller compared to a transformer with single-sided windings it also has more flux leakage, as the direction of the flux is uncontrolled. The flux leakage leads to a lower coupling coefficient, making it less efficient to use in a DIPT system [3]. To minimize the weight, the ferrite is shaped as thin rectangles instead of a full plate. This shape has been proven to still effectively guide the magnetic flux to optimize the mutual inductance [4, 29].

4.2. Coil compensation

In order to achieve higher efficiency and power transfer, coils used in DIPT systems should operate in resonance. In that case, the power transfer can be seen as purely resistive, as no imaginary components are present. This can be achieved by compensating for the inductance of the coil by using capacitors to obtain resonance [7]. The capacitors can be placed either in series or in parallel, depending on the type of compensation. One of the most widely used topologies is the series-series (SS-type) compensation, which offers a constant current output characteristic. Its compensation capacitance value is independent of both the mutual inductance and the load [15, 20]. For an SS compensation circuit with a current sourced input the output power will increase when the mutual inductance is increased whereas this is not true for a voltage sourced input [2].

4.2.1. DLCC compensation

To enhance both the stability and efficiency of systems with primary-side parallel capacitor compensation (PS-type), researchers have introduced inductive components in series into the topology. When an inductor is added on the primary side, the resulting configuration is known as the DLCC compensation topology [15]. While the extra components make the circuit less efficient under aligned conditions, the DLCC has a significant advantage in misaligned conditions. Unlike the SS-type compensation, the Tx-coil winding current is independent from the mutual inductance with a DLCC compensation circuit. The advantage is that high Tx-coil current stresses due to the fluctuation in mutual inductance can thus be avoided [20, 26, 31]. As a DIPT system often experiences misaligned conditions, the DLCC-type compensation was chosen as most suitable. The rest of this section will explain how the DLCC compensation circuit works.

The DLCC circuit is depicted in Fig. 4.4. To determine the value of circuit components, one starts with Kirchhoff's voltage law in the left most loop, making sure that this operates in resonance, to obtain Eq. 4.1.

$$C_{f1} = \frac{1}{\omega^2 L_{f1}} \tag{4.1}$$

Then Kirchhoff's voltage law in the second loop will result in Eq. 4.2.

$$C_{s1} = \frac{1}{\omega^2 (L_{\text{Tx}} - L_{f1})} \tag{4.2}$$

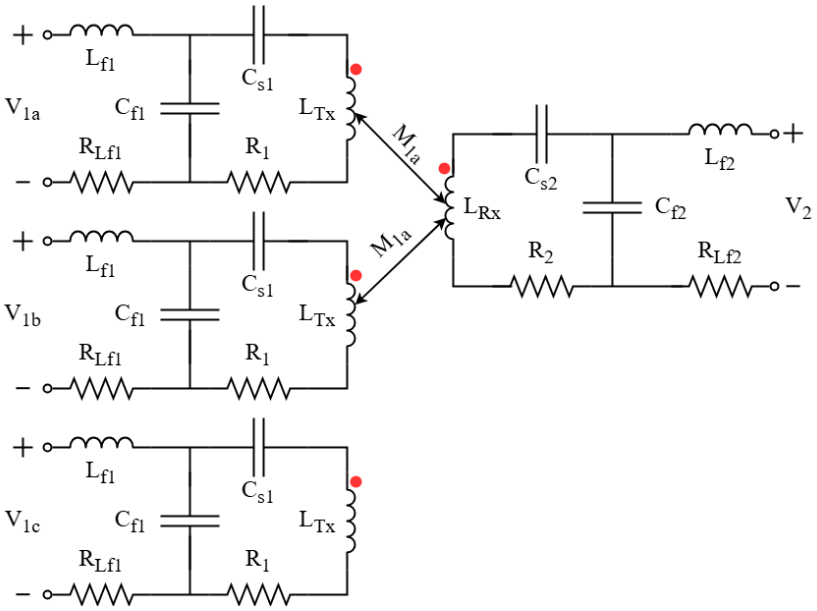

Figure 4.4: Circuit of the DLCC compensation with magnetic coupling

Note that L_{f1}, C_{f1} and L_{Tx} form a resonance tank, so the power transfer can be seen as resistive. Which means that the current through the Tx-coil is solely dependent on the RMS value of the input voltage V_{1a} and the value of L_{f1}. V_{1a} is the terminal input voltage and V_2 is the output voltage. The current through the Tx-coil can then be described as in Eq. 4.3.

$$I_{L_{\text{Tx}}} = \frac{V_{1a}}{j\omega_0 L_{f1}} \tag{4.3}$$

After this, the steps taken for the Tx-coil side can be copied on the Rx-coil side, obtaining the same results, resulting in Eq. 4.4.

$$I_{L_{\text{Rx}}} = \frac{V_2}{j\omega_0 L_{f2}} \tag{4.4}$$

Notice that in both cases, the self- and mutual (M) inductance, is no factor in either equation. That is beneficial as relative coil movement will not cause fluctuations in the coil-currents. Which is why the DLCC circuit has a higher tolerance for misalignment.

Using substitution the output current on the receiver side, $I_{L_{f2}}$, can be expressed as in Eq. 4.5. This way, the output can be seen as a constant current source, that is independent of the load resistance.

$$I_{L_{f2}} = \frac{V_a M}{j\omega_0 L_{f1} L_{f2}} \tag{4.5}$$

When the receiver side is connected to a resistive load R_{load}, the power delivered becomes as described in Eq. 4.6. From which it can be concluded that this is dependent on the mutual inductance M, underlining the need to minimize fluctuations in this parameter.

$$P_{\text{load}} = I_{L_{f2}} \cdot I^*_{L_{f2}} \cdot R_{\text{load}} = \frac{M^2 V_a^2 R_{\text{load}}}{\omega_0^2 L_{f1}^2 L_{f2}^2} \tag{4.6}$$

5

Model implementation and simulation

Given the complexity of the system, the finite element modeling (FEM) tool COMSOL is used to model the electromagnetic fields of the system of coils. The goals is to calculate the mutual inductance between one Tx- and one Rx-coil, for various x-positions of the Rx coil. The dataset will be exported to MATLAB and used to extract a graph plotting the mutual inductance against the x-position of the receiver coil. Using the same dataset, it is possible to obtain the mutual inductance curve of multiple Tx- and Rx-coils. From the obtained data-sets it is possible to construct mutual inductance and voltage graphs for the complete coil system. The final result will be two heatmaps from which the optimal coil spacing for both the Tx-and Rx-side coils can be obtained.

5.1. COMSOL

5.1.1. COMSOL model implementation

The geometric model of both coils that is used in COMSOL (*version 6.2*) is based on the specifications provided in Table 5.1. It is constructed using the magnetic fields interface from the AC/DC physics module, making use of the *"Coils"* and *"Ampere's Law"* domains that are build into COMSOL. An illustration of what the model geometry looks like is shown in Fig. 5.1, note that this does not show the domain boundaries.

Table 5.1: Coil parameters used for COMSOL modeling

Variable	Symbol	Unit	Tx / Rx
Vertical clearance	Z_{ag}	mm	50
Number of turns	N	–	20/20
Inner diameter	w_{in}	mm	44 / 44
Outer diameter	w_{out}	mm	140 / 140
Ferrite bar thickness	h_{fe}	mm	4.1 / 4.1
Ferrite bar width	w_{fe}	mm	28/ 28
Ferrite bar length	l_{fe}	mm	172 / 129
Gap between ferrite bars	w_{ag}	mm	12 / 12
Litz wire diameter	d_{a}	mm	2.4 / 2.4
Gap between coil and ferrites	g_{cf}	mm	3 / 3

Fig. 5.1 shows the Rx-coil above the Tx-coil. The coils are designed as rounded-edge squares with a cutout in the middle. The Tx-coil consists of two squares, positioned next to each other along the x-axis, forming a dual-phase coil. They are centered around $(0, 0, 0)$, with a 2 mm gap along the y-axis. Underneath the Tx-coil, three rectangles serve as a ferrite backing, which are also aligned along the x-axis. The Rx-coil is positioned 5 cm above the Tx-coil, and also centered around $(0, 0, 0)$. Similar to the Tx-coil, the Rx-coil has the three ferrite rectangles above the coil.

The materials used in the COMSOL model are air, copper, and ferrite. A full list of material properties

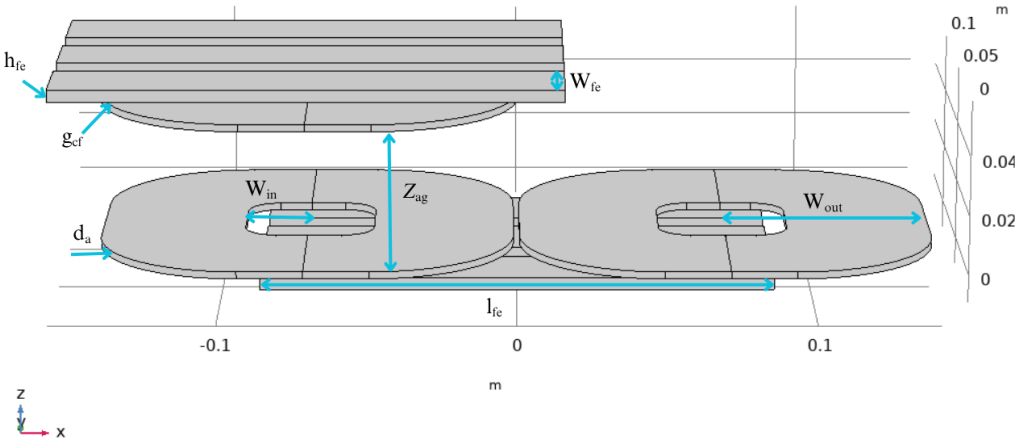

Figure 5.1: Parameters indicated for the coils with ferrite from the COMSOL model

can be found in Appendix A.2. Notably, aluminum is used to represent the used ferrite, with its relative permeability set to 4500. Additionally, the electrical conductivity of air is adjusted to 10 S/m.

A spherical domain surrounds the coils and their ferrites, with a radius five times the total length of the Tx-coil. The sphere is assigned the material property of air. The *"Magnetic Insulation"* property is applied on the boundaries of the sphere to ensure the magnetic field remains contained within its boundaries. The coils are assigned the *"Coils"* domain, whereas the air and ferrites are assigned the *"Ampère's Law in solids"* domain.

The model includes three coils, all defined as numerically homogeneous multi-turn coils. The Tx-coil consists of two such coils, each carrying a current of 5 A, in opposing direction to mimic a bipolar coil. The Rx-coil carries no current, and can thus be seen as a short-circuit.

In order to obtain the electromagnetic field in described system, first a so called *"Coil analysis"* study is performed, where after a *"Frequency domain"* study at 85 kHz results in the data used for this thesis.

5.1.2. COMSOL results

In order to verify the model, the value of the self inductance for the Tx-coil is compared to the measured value found in Table A.1. To obtain the mutual inductance in COMSOL, the *"Self Inductance"* variable is used in the derived values values section. In Table 5.2 the results from the COMSOL simulations are shown, as well as measurements performed using an LCR-meter, which will be discussed in Chapter 7.

Table 5.2: Measured and calculated values of the coil self-inductances

Variable	Symbol	Unit	Measured	COMSOL
Tx-coil	L_{Tx}	μH	121.6	133.3
Rx-coil	L_{Rx}	μH	56.06	59.3

From these results it can be concluded that the measured value is significantly lower than the values determined in COMSOL. However, it is only 9.6% . However this can be attributed to the (in)accuracy of the measurements, and to the geometry of the COMSOL coils being a ideal rounded square, which is not the case for the real coils. Due to this, the COMSOL model is deemed accurate enough for further use.

The mutual inductance is then calculated using Eq. 5.1 in the derived values section of COMSOL. The Rx-coil voltage has both a real- and imaginary part, the first being due to the coil resistance, and the latter to the reactance, thus both the coil inductance as its parasitic capacitance. The influence of the latter decreases with frequency, opposite from the increasing inductive part. Therefore, when using a

relatively high frequency of 85 kHz, it can be assumed that the imaginary part of the coil voltage is due to the coil inductance.

$$L_{\text{mutual}} = \frac{V_{\text{Rx}}}{2\pi f_0 I_{\text{Tx}}} = \frac{\text{Im}(\texttt{mf.VCoil\_Rx})}{2\pi f_0 \cdot \texttt{mf.ICoil\_Tx1}} \tag{5.1}$$

To plot the mutual inductance against the varying x-position, a dataset is extracted using a parametric sweep. This sweep changes variable `x_offset`, which is used to determine the position of the Rx-coil and the ferrites attached to it. The parametric sweep runs from 16 cm to the left of the Tx-coil to 16 cm to the right of the Tx-coil, with steps of 1 mm. For every step and thus (relative) position, the mutual inductance is then calculated using Eq. 5.1.

This resulted in the plot shown in Fig. 5.2. The plot shows a peak at `x_offset = -0.068 m` with a maximum mutual inductance of 22.4987 μH and a dip at `x_offset = 0.068 m` with a minimum mutual inductance of -22.4979 μH. The peak should be when the Rx- and Tx-coil are perfectly aligned. That is when Rx-coil has an offset of $\pm$2 mm from the center, thus $\pm$0.068 mm total x-axis displacement. Also note that the mutual inductance changes sign when the Rx-coil moves further away from the Tx-coil along the x-axis, this is explained by change in direction of the magnetic flux field generated by the Tx-coil as the distance increases, which can be seen in Fig. 5.3. in conclusion, the result is as expected, and the obtained dataset can be further processed in MATLAB.

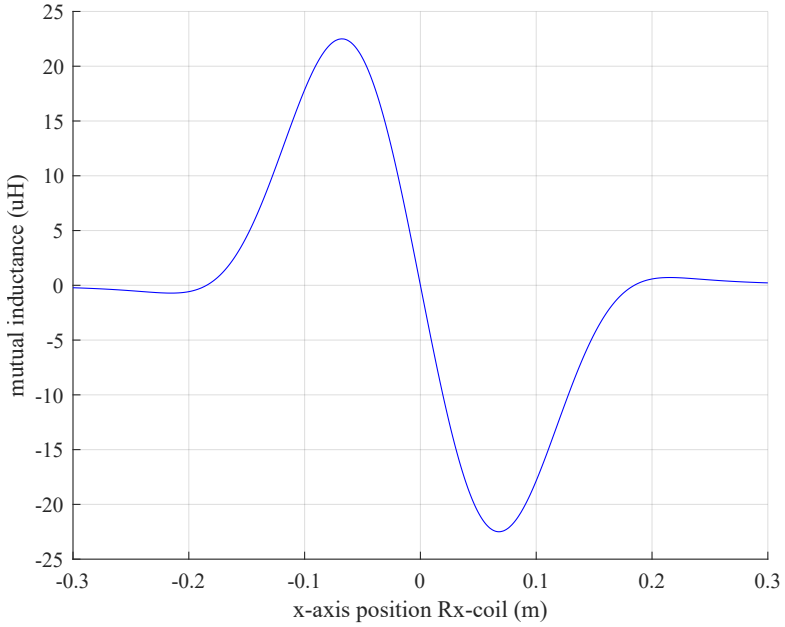

Figure 5.2: Plot of the mutual inductance against different x-positions from the COMSOL data

5.2. MATLAB

For a system of multiple coils, the total mutual inductance can be calculated from the mutual inductance values between all Tx- and Rx-coils according to the superposition principle [11, 30]. By multiplying and phase shifting the COMSOL data set, the system can be modeled for two Rx- and multiple Tx-coils. By doing it in this manner, time consuming computations by COMSOL are avoided, as applying FEM to a system of multiple coils requires heavy computations.

5.2.1. MATLAB multi-coil model implementation

To make the COMSOL data-set usable for further MATLAB computations, it is first trimmed and zero-padded. As the COMSOL model only takes one set of coils into account, the data at both ends of the data-set in Fig. 5.2, are deemed incorrect.

Since the Tx-coil is centered around zero and has a length of 0.28 m, the region of overlap and thus correct mutual inductance, is at least from -0.14 m to 0.14 m, along the x-axis. Once the mutual

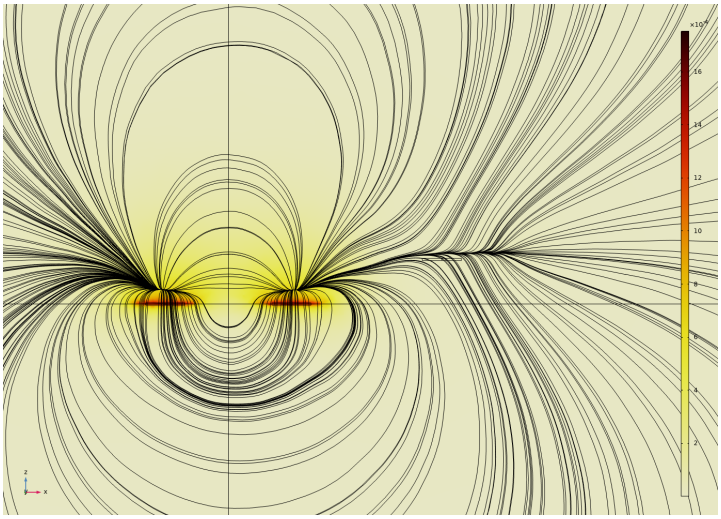

Figure 5.3: Illustration of the flux lines from the Tx-coils in COMSOL, with the Rx-coil to the right of the Tx-coils

inductance reaches zero at -0.185 m, it crosses zero and flips sign. The same happens at the other side, and should in both cases be avoided. The trimming is done by deleting all points after the mutual inductance crosses the zero point on both edges of the Tx-coil. After this, the data is zero-padded which will allows the use of superposition in a circular manner. The resulting mutual inductance curve forms the basis of all further computations.

The next step is to transpose the mutual inductance curve to the location of the other Tx-coils. For illustration purposes this is shown for three Tx-coils in Fig. 5.4. The Tx-coils are evenly spaced and shifted with *Tx-gap*, to both the left and right side of the original Tx-coil. In the MATLAB script found in Appendix B in Section B.1, the shift is done with the variable *"Tx-spacing"*. This results in two new 2D array's, for both Tx-coils, containing a mutual inductance curve for each value of *"Tx-spacing"*. These are then linearly added together with the original Tx-coil data, obtaining an array for the total mutual inductance data for three Tx-coils and one Rx-coil.

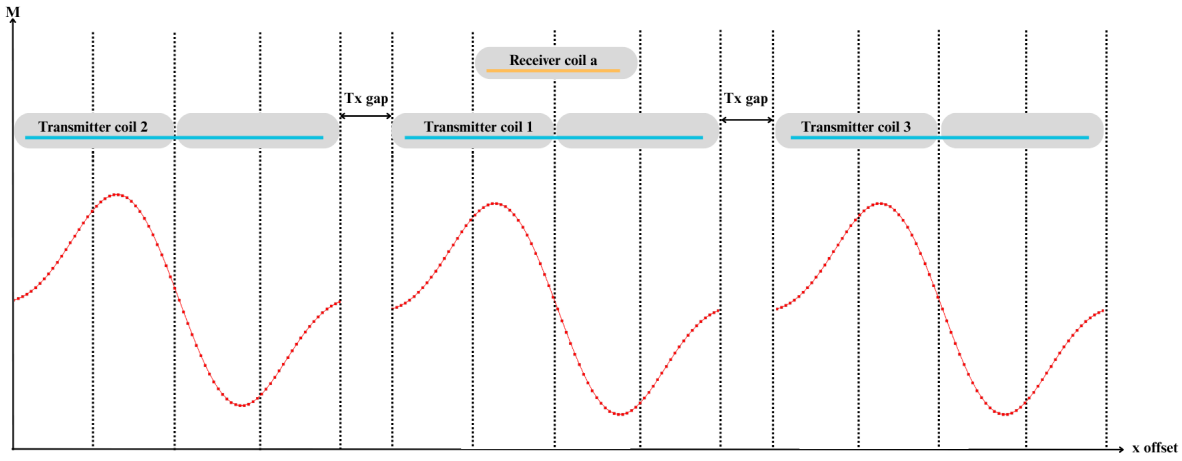

Figure 5.4: Mutual inductance linearly transposed for a three Tx-coils

The same process of shifting and addition is then repeated for adding a second Rx-coil. Starting simple, Fig. 5.5 shows how the Rx-spacing affects the data for a singular Tx-coil. When the Rx-coil *"b"* is in the middle of first Tx-coil, there is zero mutual inductance. The curve shows the mutual inductance when the two Rx-coils, connected in series aiding, move over the Tx-coil, with `x_offset` indicating the relative placement.

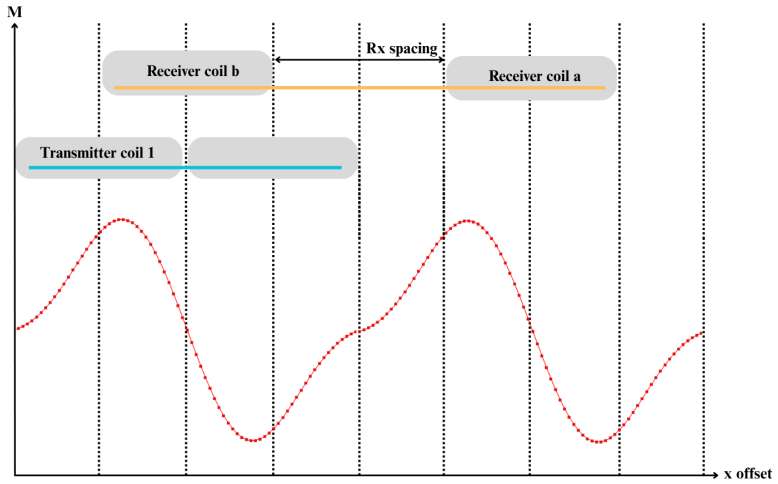

Figure 5.5: Mutual inductance linearly transposed for a second Rx-coil with only one Tx-coil

In the MATLAB script this shifting is performed using the curve of all three Tx-coils instead of a singular Tx-coil. The shifting is done with a nested loop, resulting in a 3D dataset, as now the *"Rx-spacing"* variable is also introduced. In Fig. 5.6 an illustration is shown of two Rx- and two Tx-coils. The red curve shows the mutual inductance for Rx-coil "a" and the green curve shows the mutual inductance for Rx-coil "b", both against their relative position to the Tx-coils 1 and 2.

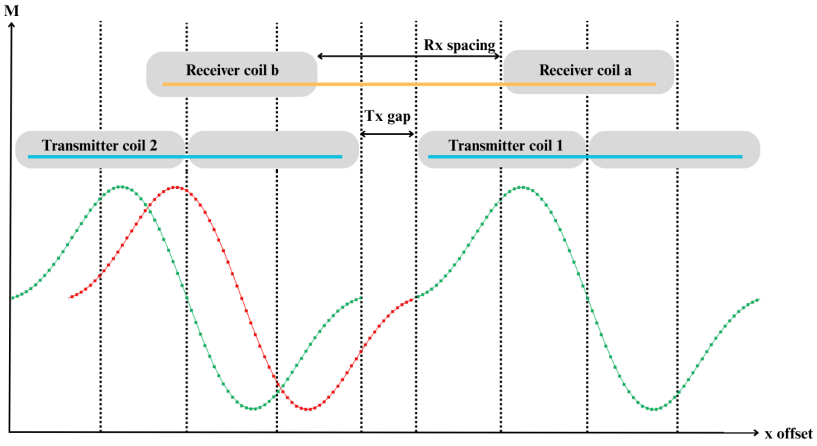

Figure 5.6: Mutual inductance between Tx-coils and Rx-coil "a" (red), and Rx-coil "b" (green)

5.2.2. MATLAB multi-coil results

The original MATLAB script uses three Tx-coils and two Rx-coils, which should be sufficient to determine the optimal coil spacing. However, the tests performed in Chapter 7 used four Tx-coils. Moreover, the testing revealed the crucial insight that the Rx-coils can be connected in series aiding or opposing aiding. The MATLAB code used to find the optimal coil spacing did not take these two facts into account. For verification purposes the MATLAB code was rewritten to confirm the test data, and include these two factors.

Extending the MATLAB to include a fourth Tx-coil was easily implementable as extendability was a system requirement. The fourth coil is implemented in Appendix B.9. Nevertheless, there is one problem with this method, as the spacing becomes to far apart there, the data-set is too short and the data loops around. A solution for this is discussed in Chapter 9. For the tested spacing the MATLAB code can run the implementation of fourth coil. Two verification plots were made to show the difference between the

three and four Tx-coil system which are shown in Fig. 5.7.

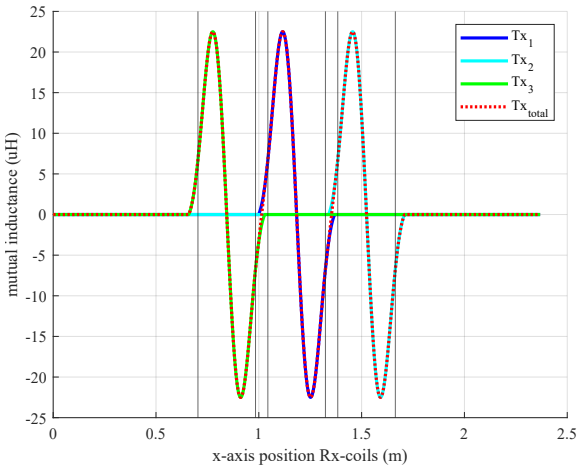

(a) Three Tx-coils system: addition of two Tx-coils

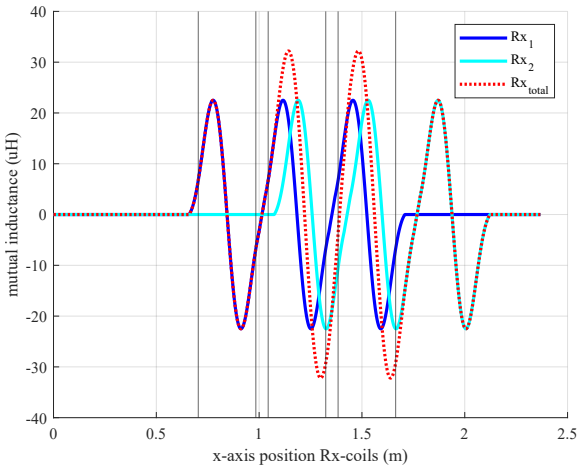

(b) Three Tx-coils system: addition of second Rx-coil

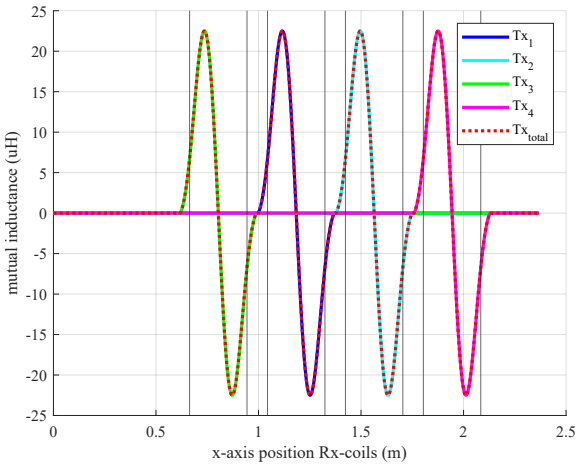

(c) Four Tx-coils system: addition of three Tx-coils

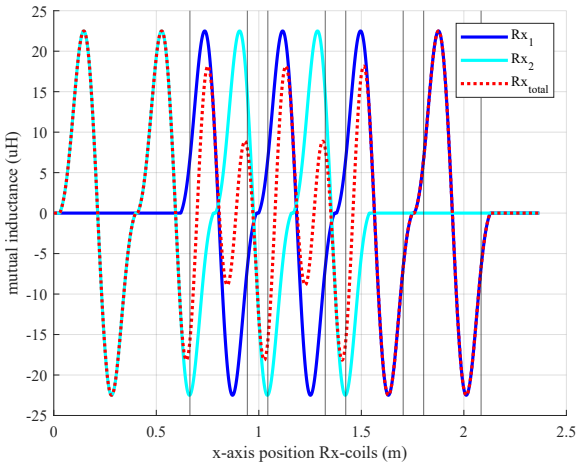

(d) Four Tx-coils system: addition of second Rx-coil

Figure 5.7: Steps showing the addition of Rx- and Tx-coils, and their mutual inductance curves for both three and four Tx-coils configurations, the black dotted lines are the edges of the Tx-coils. Note that the in (d), the Rx-coil is added to the left instead of right

Lastly, the MATLAB code was changed to include the different coil connection configurations. Section 3.1 describes how the self, and mutual inductance with series opposing versus aiding works. However, this reasoning is not applicable for this situation, as the two Rx-coils both have a mutual inductance with the Tx-coils. Due to this, a voltage on the Rx side is produced, and a current will run through the two coils. The current produced in the Rx-coils runs in the same direction for series aiding, but in the opposite direction for series opposing. So the mutual inductance curves are to be added for the series aiding, and subtracted for the series opposing.

Part of the MATLAB script from Appendix B.9 is shown in Listing 5.1 to aide the explanation for the changes that are needed. In step 3, the data set gets a minus in front as to inverse the sign of the data, then the data is shifted to the left. The inverse sign is how the Rx-coils are changed from series aiding to series opposing.

```
1           %step 3:
2           rx2_data(:, n, k) = circshift(-rx1_data(:, k), -rx_coil_shift);
                %shift Rx1-data to Rx2-coil
```

Listing 5.1: Step 3: Shifting Rx1 data to Rx2 coil

Fig. 5.8 shows the different outputs of the mutual inductance when the Rx-coils are either in series opposing or aiding. From this it can be concluded that if the coils are placed connected in series opposing, a dip in the absolute mutual inductance forms whilst the series aiding configuration does not show this behavior.

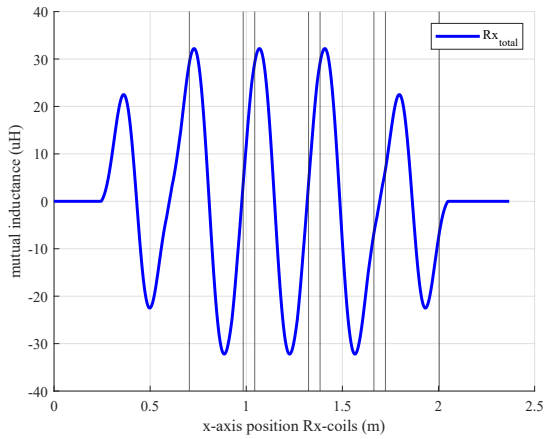

(a) Mutual inductance curve with 4 Tx-coils and 2 Rx-coils in series aiding

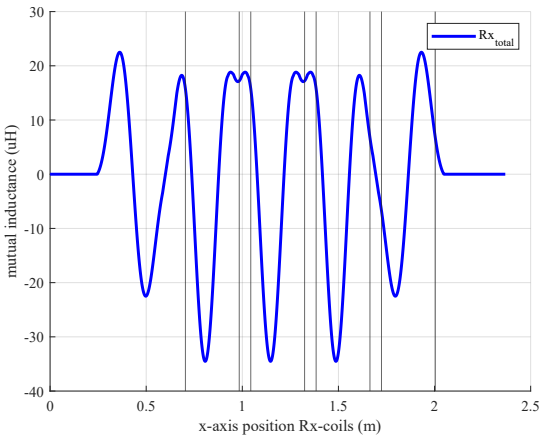

(b) Mutual inductance curve with 4 Tx-coils and 2 Rx-coils in series opposing

Figure 5.8: Mutual inductance curves for series aiding and opposing

6

Optimizing coil spacing

To minimize the overall system power fluctuation, the optimal spacing for both the Tx- and Rx-coils will be determined using the data obtained in Chapter 5. The system of coils with the two spacings that have to be optimized are illustrated in Fig. 6. The optimal coil spacing is where the average voltage is the highest whilst the fluctuation in voltage is kept the smallest across the x-axis trajectory. The following chapter will continue with MATLAB to obtain two heatmaps on these parameters from the system, and determine the optimal coil-spacings.

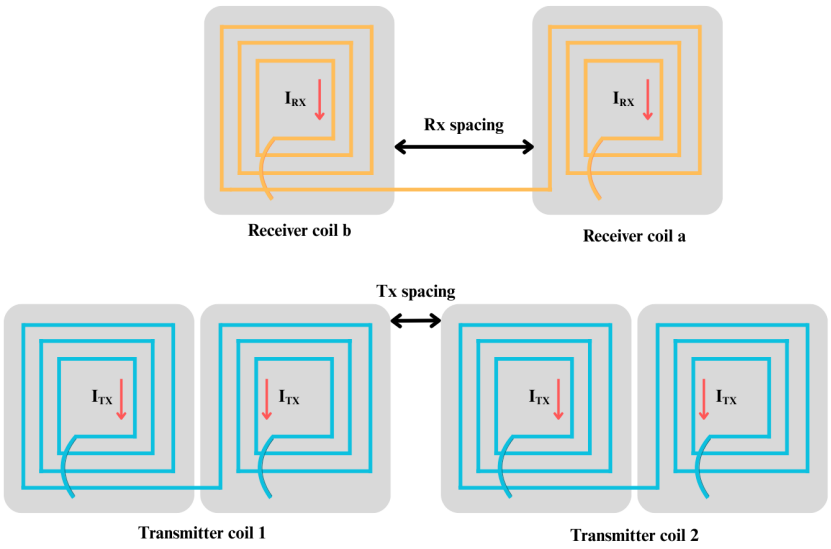

6.1. MATLAB heatmap implementation

To find the optimal coil spacing for both the Rx- and Tx-side coils, the average value, and the fluctuation of output voltage is required for each unique combination of Rx- and Tx-spacing. Before calculating these, the data-set of the total mutual inductance, resulting from Chapter 5, has to be trimmed. This is done as only the truly periodic part of the mutual inductance curve should be used, as for the real world application the number of Tx-coils is larger. The index range for this is determined by finding the points were the mutual inductance is non zero for both Rx-coils, then selecting the points that start the latest and end the earliest.

Fig. 6.1 shows the resulting mutual inductance curve from the MATLAB script with a given *"Tx- and Rx-spacing"* for the complete system, consisting of three Tx-coils and two Rx-coils. The black lines display the edges of the Tx-coils. The figure highlights the part of interest between the red lines, where the two Rx-coils completely overlap with the the Tx-coils. The system with numerous Tx-coils will be periodic with this part of the curve. As the second Rx-coil is placed to the right of the original one, the part of interest thus coincides with the curve on the center and right side Tx-coil. In Chapter 6, this curve is trimmed to aforementioned part for further use.

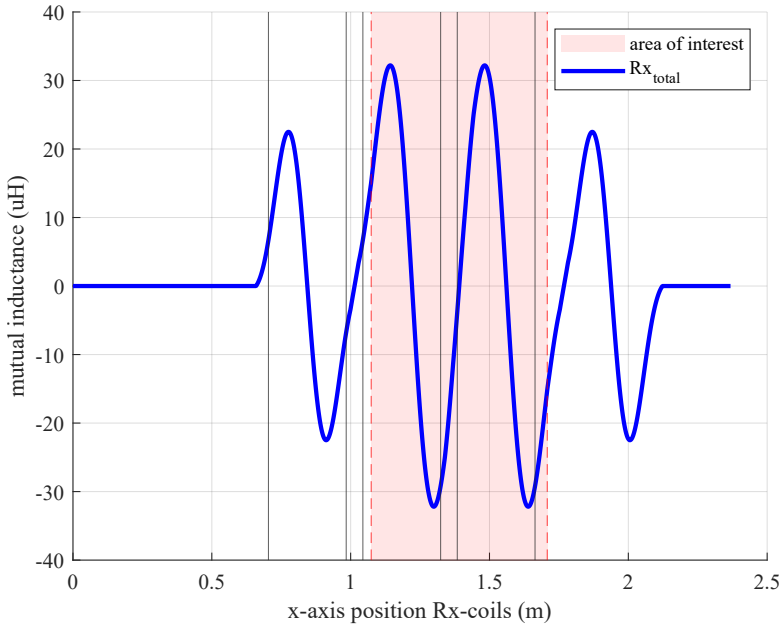

Figure 6.1: Overall system mutual inductance curve for *Tx-spacing* = 6 cm and *Rx-spacing* = 27.4 cm, for three Tx coils and two Rx coils

From this mutual inductance curve, the voltage curve is calculated by using Eq. 6.1.

$$V_{\text{Rx}} = L_{\text{mutual}} \cdot 2\pi f_0 I_{\text{Tx}} \tag{6.1}$$

Then the voltage fluctuation can be calculated by taking the absolute difference over the curve using Eq. 6.2.

$$\Delta V_{\text{Rx}} = \frac{\max\left|V_{\text{Rx}}(x)\right| - \min\left|V_{\text{Rx}}(x)\right|}{2} \tag{6.2}$$

Next, the average voltage is determine by using the integral as shown in Eq. 6.3. Where, $x_{\text{t}} = 1.184$, is the physical length of a period of voltage curve.

$$\text{avg}\left[V_{\text{Rx}}\right] = \frac{1}{x_{\text{T}}} \int_0^{x_{\text{T}}} V_{\text{Rx}}(x)\, dx \tag{6.3}$$

6.1.1. Results

The first heatmap of interest is shown in Fig. 6.2. The figure shows the lowest voltage fluctuation in black and the highest voltage fluctuation in white. The goal is to minimize the voltage fluctuation, therefore the ideal spacing is where the figure is the darkest.

Another performance indicator is the average voltage, plotted on a heatmap in Fig. 6.3. In contrast to the previous heatmap the optimal parts are now the lightest color, as the average voltage is the highest for these coil spacing combinations. As can be seen, the area of overlap is non existent. Concluding that the proposed system cannot reduce the voltage fluctuations.

To confirm this conclusion multiple mutual inductance curves were plotted. None were able to avoid zero crossings. Concluding that this implementation also fails to uphold the requirement specification that the mutual inductance between the Tx and Rx-side must never be 0 H.

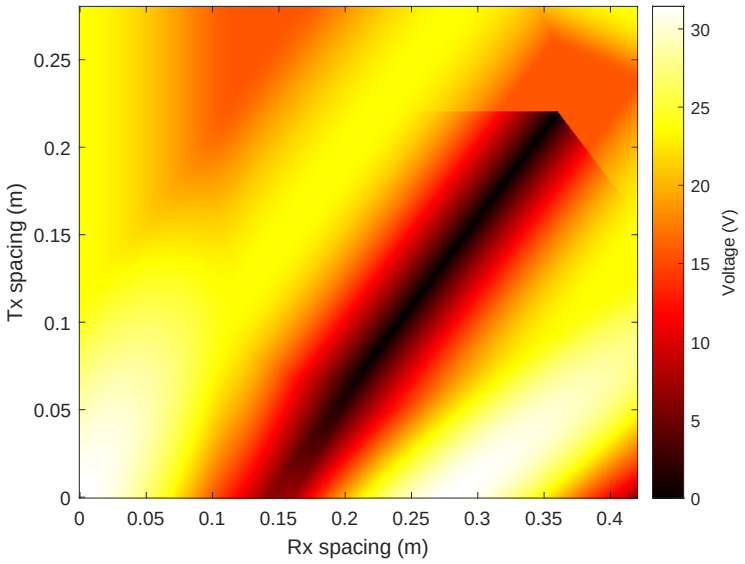

Figure 6.2: Heatmap of the voltage fluctuation for all combinations of Tx- and Rx-coil spacing

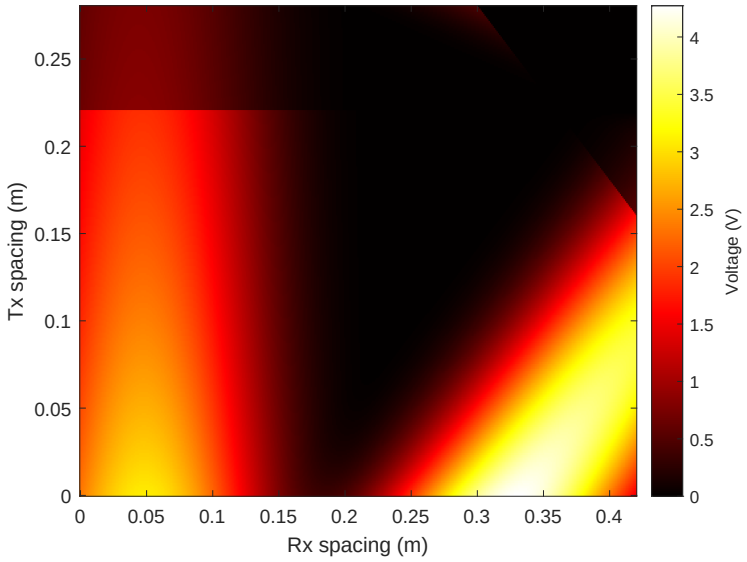

Figure 6.3: Heatmap of the average voltage for all combinations of Tx- and Rx-coil spacing

7

Testing and verification of results

The testing for this thesis aims to obtain a data-set regarding the mutual inductance of the DIPT system, without the compensation circuit, to verify the model and simulations performed. Two tests are conducted to measure the mutual inductance for various relative x-positions. The first test measured the mutual inductance between one Tx- and one Rx-coil, the second test measured the mutual inductance for two Rx- and four Tx-coils. A third test looked into the output voltage of the system.

The first test should verify the COMSOL model simulations on mutual inductance versus trajectory, the second test should verify the MATLAB model. When these are both verified, the model for finding the optimal coil placement will be proven to be based on accurate data, and thus deemed valid. The last test shows what the output voltage of the system is. This chapter will explain the experimental setup, procedures, and present the results, comparing them against the COMSOL simulations and MATLAB model.

7.1. Test setup

All tests were performed in an aligned condition with respect of the y-direction. A side-view of the x-position is shown in Fig. 7.1. It shows how the x-positions of the coils are related for two Rx-coils and two Tx-coils. The equipment needed for the tests is almost identical for both the first and second test,

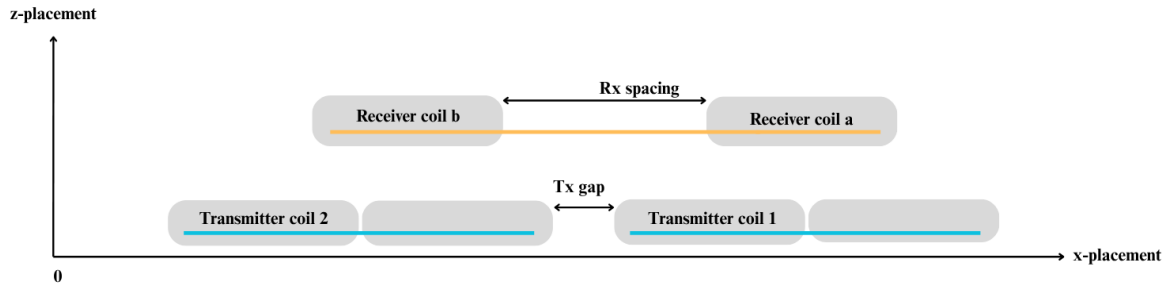

Figure 7.1: Test setup illustrating the relative x-positions of the coils for a two Rx- and two Tx-coil configuration

except for the number of coils. The first test uses one Tx-coil and one Rx -coil. The minimal measuring length is the length over which the Rx-coil has to at least pass to have data comparable to COMSOL. This is equal to the length of the Tx-coil, $2 \cdot 0.14 = 0.28$ m. As there will be a gap between the Tx-coils, the measurement will be performed over 0.40 m. This also allows for a set of measurements when the Tx- and Rx-coils are not aligned. The mutual inductance will be measured at intermediate points with a distance between them of 5-10 mm.

The second test measures the mutual inductance for an Rx-coil spacing of 0.274 m and a Tx-coil spacing of 0.060 m. The minimal measurement length required to pass over all four Tx-coils with at

least one Rx-coil can be calculated as $0.274 \cdot 3 + 4 \cdot 2 \cdot 0.140 = 1.3$ m. For these measurements, especially the middle part is of importance, thus measurement are started in the middle. This part is most important, as this is where both of the Rx-coils are passing above the Tx-coils. In general larger DIPT system this is most of the times the case, as the amount of Tx-coils will be significantly larger. The mutual inductance will again be measured at intermediate points with a distance between them of 5-10 mm.

For the testing the following equipment is needed:

- The xyz-gantry: to precisely measure the position.
- Two Rx-side receiving coils: used to measure the mutual inductance.
- 4 Tx-side bipolar transmitting coils: these simulate the 'charging surface' over which the Rx-coil will move.
- LCR-meter HM8018: to measure the self- and mutual inductance of the coils.

The equipment is connected as depicted in Fig. 7.2 for test scenario 1, and connected as depicted in Fig. 7.3 for test scenario 2. The LCR meter is connected to the Tx- and Rx-coils in series as explained in Chapter 3. The LCR meter determines the inductance from the magnitude and phase difference between the resulting voltage and current. This is used to determine the real and imaginary part of the impedance, where the inductance is the imaginary part of this impedance, as the frequency used is high enough to deem the parasitic capacitance insignificant. The frequency that is be used in the final design is 85 kHz. However, the LCR meter will be set to 25 kHz, as this is its highest setting. This is in the mid-frequency (10 kHz – 100 kHz), meaning that setting LCR meter at 25 kHz will not result in a significant parasitic capacitance that will undermine the accuracy of the measurement if the design is later coupled to 85 kHz [1, 19].

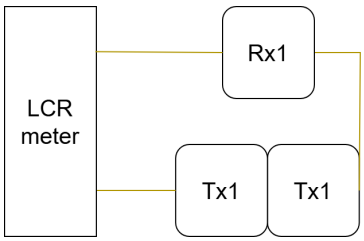

Figure 7.2: Schematic illustration for the test setup of scenario 1

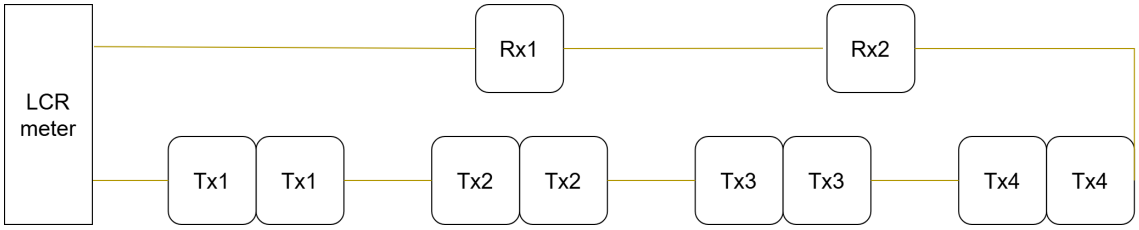

Figure 7.3: Schematic illustration for the test setup of scenario 2

The third test measures the output voltage. To do this the test setup is changed, Fig. 7.4 shows the new test arrangement. The test still uses the xyz-gantry, two Rx-coils and four Tx-coils. However, to measure the output voltage, the LCR meter will not suffice. Instead a power supply with a DC input of 50 V is connected to an inverter which produces an AC wave with an operating frequency of 85 kHz. The inverter is connected to each Tx-coil separately with the compensation circuit in between. On the receiver side the coils are connected in series with the compensation circuit, which is connected to an oscilloscope, with a converter in between the two. The voltage is then be measured over a load resistance of 50 Ω. During the test the Rx-coils will move over the Tx-coils to obtain the voltage over time, and thus space.

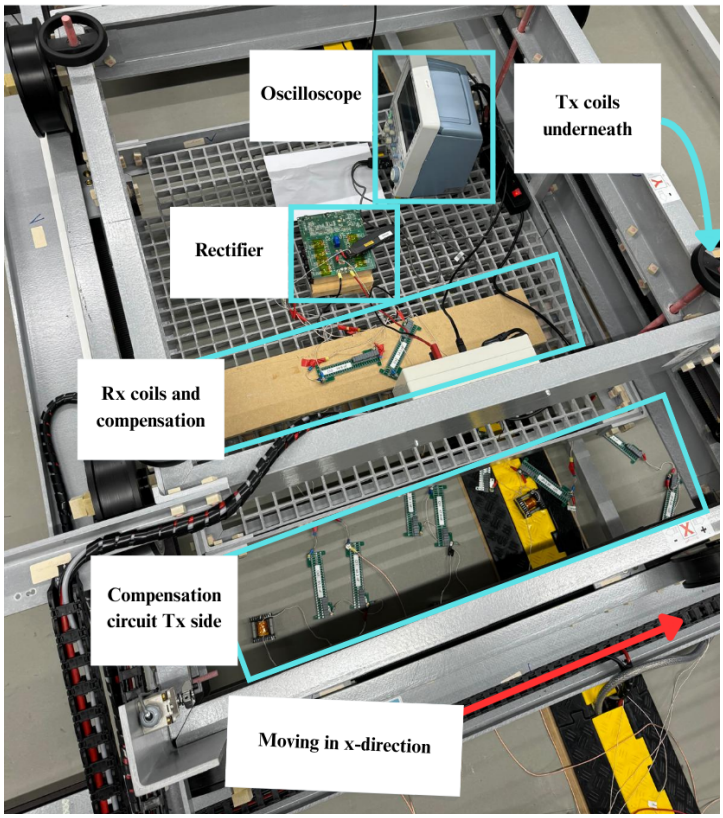

Figure 7.4: Photograph of the test set up of scenario 3

7.2. Test results

To compare the test results with the COMSOL simulation and the MATLAB model, it is necessary to measure the self inductance and the xyz-position of the coils. The self inductance is tested by placing a single coil in series with the LCR meter, away from any metal, thus also from the other coils. One encountered problem is that the Tx-coils are glued together at a set distance of 6.0 cm. For the xyz-position, the x-position is moving and will be measured at each point using a laser. The y-position is precisely aligned to Tx-coils, therefore it is not recorded.

The z-position determines the vertical spacing between the Tx- and Rx-coils. This gap is a crucial parameter for the mutual inductance. The first simulations of the COMSOL model are performed with a gap of 5.0 cm, during the testing the gap was measured to be 5.6 cm. For this reason, the COMSOL simulation is run again with a gap of 5.6 cm to ensure an accurate comparison of the data. The measurements results are recorded in Table 7.1. The new COMSOL simulation gave a result which was only 4.58 % higher than the measured value.

Table 7.1: Comparison of the predictive COMSOL simulation, test measurement, and adjusted COMSOL simulation

Parameter	Unit	COMSOL	Test	2nd COMSOL
Inductance Tx	μH	133.3	124.1	129.78
Inductance Rx	μH	–	56.06	–
Mutual inductance max	μH	22.5	14.42	19.04
Mutual inductance min	μH	-22.5	-14.58	-19.04
Vertical spacing	cm	5.0	5.6	5.6
Spacing Tx-coils	cm	–	6.0	–
Spacing Rx -coils	cm	–	27.4	–

7.2.1. First test

The results of the first test shows a mutual inductance curve similar to that of the COMSOL model, as illustrated in Fig. 7.5. Although, the two graphs show different maxima and minima for the mutual inductance. The COMSOL data gives a maximum mutual inductance of 19.04 μH, while the test scenario shows that the maximum inductance is 14.42 μH. Similarly, the minimum for the COMSOL data is at -19.04 μH, whereas the test measures -14.58 μH. The difference in values is 32.04 % and 30.59 % respectively. This is far outside the performance requirements of 10 % accuracy.

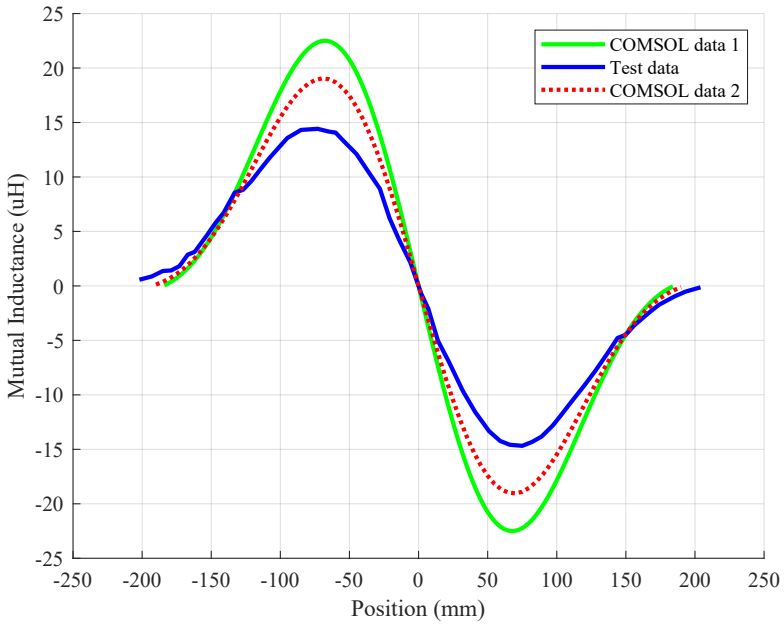

Figure 7.5: Mutual inductance data plotted against x-position, for the testing-, and both COMSOL data sets

This difference can be caused by multiple factors. Firstly, the self inductance of the COMSOL models are also above the self inductance of the test measurement. This discrepancy in self-inductance could propagate to differences in mutual inductance, as the self-inductance values are critical values for the mutual inductance. The simulation is also affected by a number of things such as the mesh resolution, material properties, and the space which is evaluated. Secondly, there exists interferences from the wires used in testing which can cause a lower inductance. A last factor could be the accuracy of the LCR meter, for mid range frequencies LCR meters have a accuracy of around 0.1 % to 0.5 % [1].

A second observation is that the curve for the tested data is not entirely smooth. This is measurement error likely is caused by human error, or interference caused by the connecting wires. While additional data points or repeated measurements could refine the curve, the current results still demonstrate a satisfactory amount of data to compare the COMSOL model to within the given experimental constraints.

7.2.2. Second test

The second test shows a more peculiar curve, depicted in Fig. 7.6a. While the MATLAB code shows an output of a (close to) sinusoidal wave, the test result appears to consist of two wider and differently sloped peaks. There are four vertical lines plotted, which indicate where these peaks occur. The peaks in this shape can only happen when the Rx-coils are in different phases. To confirm this hypothesis, the MATLAB script is rewritten so the coils are now in the series opposing configuration, as well as adding a fourth Tx-coil, as in Appendix B.9 and B.12. The script results in Fig. 7.6, which shows a graph quite similar to the test results depicted in Fig. 7.6a.

The peaks are not an exact match in value, which can be explained by an inaccurate measurement of the impedance by the LCR meter. Also note that to better match the graph of the tested data, the Tx- and Rx spacing was adjusted with a few mm in the MATLAB script. There might be an even better ratio, such that the graphs match even better and the peak might be more similar. This leads to a second dimension that the heatmap does not explore but could easily be applied; is there a better coil

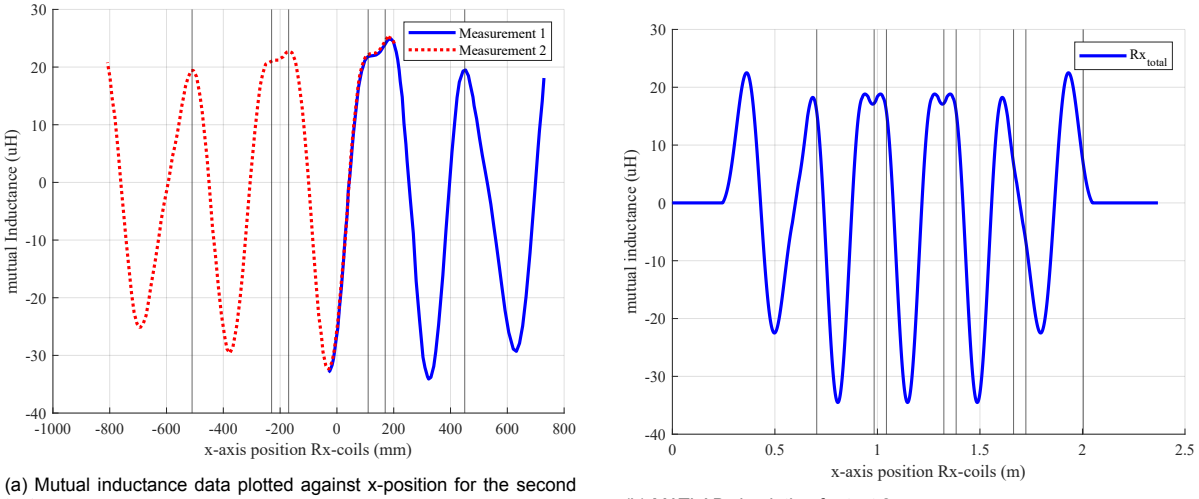

(a) Mutual inductance data plotted against x-position for the second test

(b) MATLAB simulation for test 2

Figure 7.6: Comparison between measured and simulated mutual inductance data for the second test

placement possible for opposing Rx-coils? Another interesting idea would be to look into a dual phase Rx-coil system. Which would allow even more complex combinations for the design configuration.

As the result of this adjustment shows a better similarity to the test data, it could indicate a measurement error in the spacings. As the first peak of the measured data is at 19.72 μH and the simulated value is at 18.14 μH, giving a difference of only 8.01 %. Where the individual coil test falls far outside the required accuracy range of 10 % the second test stays within these bound. This gives a strong indication that the the interference from the other Tx-coils caused the rather large error.

7.2.3. Third test

The third test shows the output voltage of the system whilst moving over all Tx-coils in the x-axis. The output voltage is heavily influenced by the mutual inductance fluctuations. However, the compensation circuit, load impedance, and rectifier also have a significant effect on the final output. The most important difference is that the voltage is always positive, so it is more similar to the absolute value of Fig. 7.6a than to the actual curve. That would mean that the expected graph of the voltage would first have four peaks, then an oddly shaped peak, a normal one, and another oddly shaped peak, followed by four more regular peaks. The actual output is depicted in Fig. 7.7, which shows the voltage output in green measured over a load impedance of 50 Ω. Note that it deviates from the expected curve, as the testing started with the Tx- and Rx-coils overlapping. Which explains why the green curve only shows two regular peaks before the first oddly shaped peak. The highest peak is at 20.2 V and the lowest at 0 V.

7.3. Conclusion

The first test did not completely verify the data from the COMSOL model. The result did show a similar curve for the mutual inductance versus the x-position between one Tx-coil and one Rx-coil. Furthermore, taking into account that the self inductance of the Tx-coil is also lower in the COMSOL model, the vertical gap between the Tx- and Rx-coil is adjusted to 5.6 cm. This significantly improved the accuracy. However, the minimal and maximal mutual inductance are 30.59 % to 32.04 % lower in real life than the simulation, which means the model fails to comply with the accuracy specification of 10 %. The second test revealed some strong indication that this large error was likely caused by the inductance of nearby Tx-coils.

The second test also revealed that the coils are connected differently than the MATLAB simulations assumed. Two oddly sloped peaks in the curve made it apparent that the Rx-coils are connected in a series opposing configuration, in contrast to the assumption that they would be connected both with the windings in the same direction. To confirm this assumption, the MATLAB script is rewritten in accordance, and a fourth Tx-coil is added. While the final graph is not an exact match, it did confirm

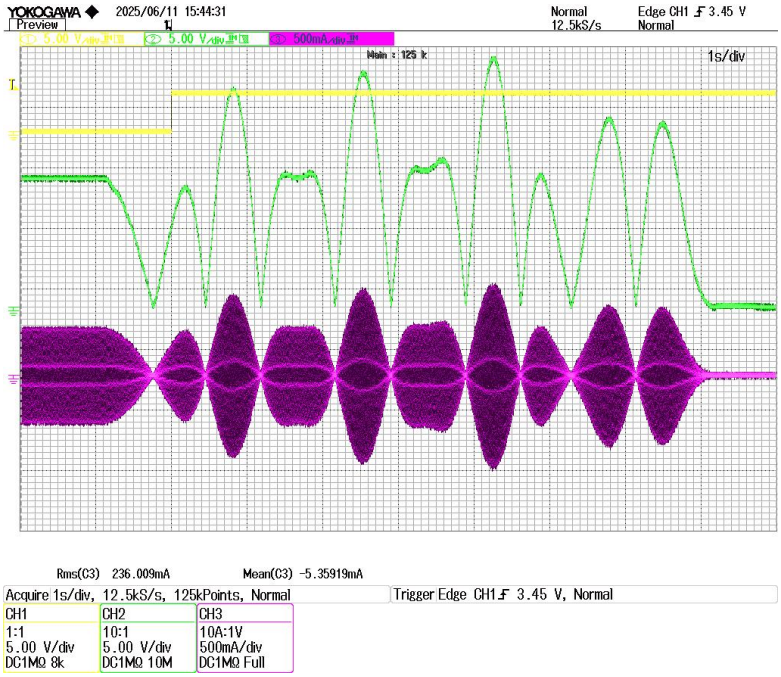

Figure 7.7: Voltage output (in green) from the third test

that the Rx-coils were connected incorrectly. In addition, a comparison of the first peak showed that the simulated data is now 8.01 % lower than the measured data.

The third test showed that the output voltage has a curve similar to that of the mutual inductance. The highest peak is at 20.2 V and the lowest at 0 V.

Overall the experiments confirm the general behavior predicted by the COMSOL simulations and the MATLAB model. They also reveal insights that lead to further adjustments to the system, improving its accuracy. These verified models can now be confidently used for further design and analysis of the DIPT system.

8

Double Rx side system

Chapter 6 concluded that a system with the Rx coils in series does not reduce the mutual inductance fluctuation. A better solution could be to also use double phase receiver side coils. The coils are then individually connected to their own compensation circuit and AC to DC converter before they can be connected in parallel. The proposed system is illustrated in Fig. 8.1. The parallel design could allow the coils to have an output voltage without zero crossings. As the voltage at the output of the rectifier is a positive DC signal, also shown in test 3 described in Chapter 7. That means it is possible to configure the coils in such a way that the output voltage will no longer have zero points when the Rx-coils are within the Tx-coil track.

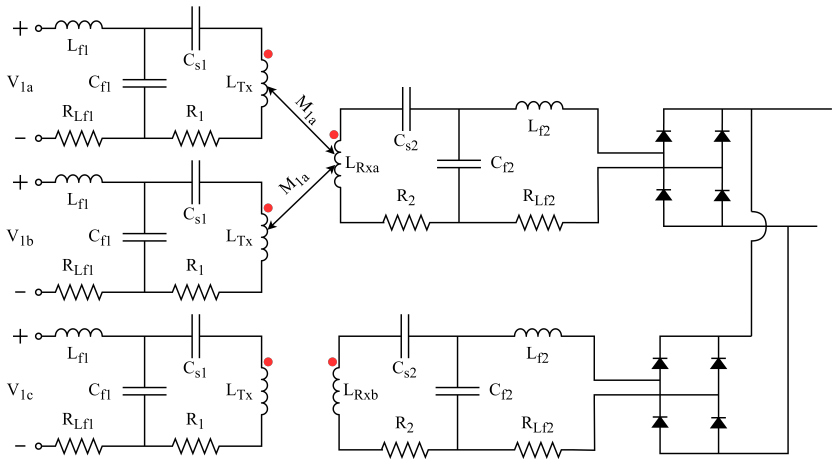

Figure 8.1: The circuit design of the proposed double Rx side system.

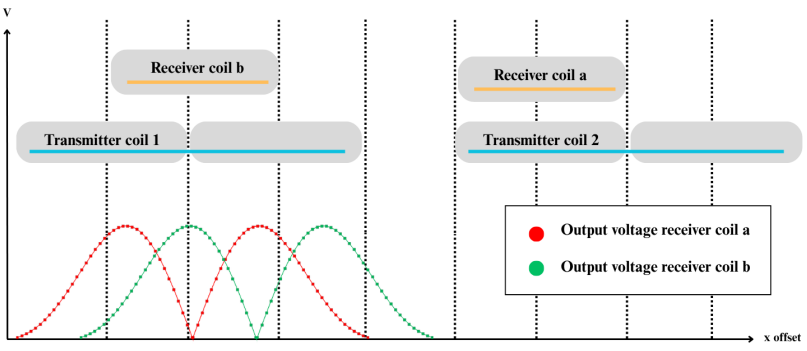

Figure 8.2: Voltage output of the double Rx-coil side summed

The zero crossings in the output voltage could be avoided when the circuit is connected in parallel, as the output voltage will be summed, resulting in Fig. 8.2. The figure shows the two output voltage curves. When Rx-coil ”b” is in the middle of Tx-coil 1, the voltage will be 0 V. With the Rx-coil ”a” on top of Tx-coil 2, the voltage is at its peak. The figure overlaps the two curves at this particular time instant to show how the 0 V points can be avoided.

To determine the optimal spacing the MATLAB script was changed to calculate the the voltage of both the Rx-coils separately. The changes were only applied to the main script, and a new script was made to plot the output voltage. The new scripts are attached in the Appendices B.11 and B.10. With these changes, two new heat maps can be plotted to find the optimal coil spacing.

The first heatmap, depicted in Fig. 8.3, shows the the average voltage for different Tx- and Rx-coil spacings for the double Rx side system. The second heatmap illustrated in Fig. 8.4, shows the voltage fluctuation for different Tx-and Rx-coil spacings for the double Rx side system. The optimal spacing is where the average voltage is the highest whilst having the lowest voltage fluctuations. The two blue circles indicate the optimal spacings, placed at the points that overlap the highest average voltage and the least amount of voltage fluctuation.

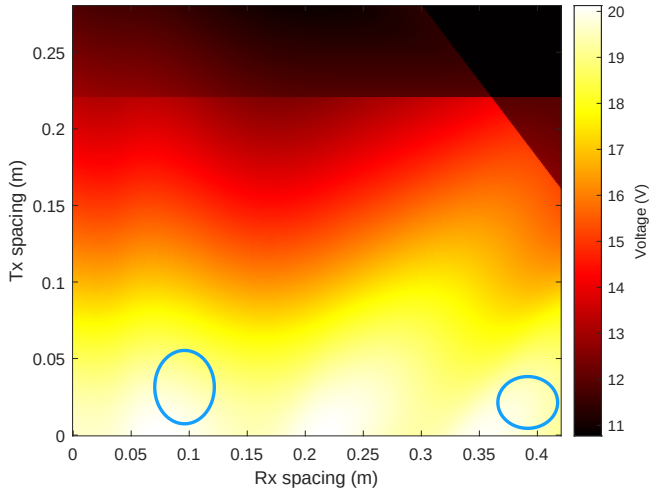

Figure 8.3: Heatmap showing the average voltage for different Tx- and Rx-coil spacings for the double Rx side system. The two blue circles indicate the optimal spacings

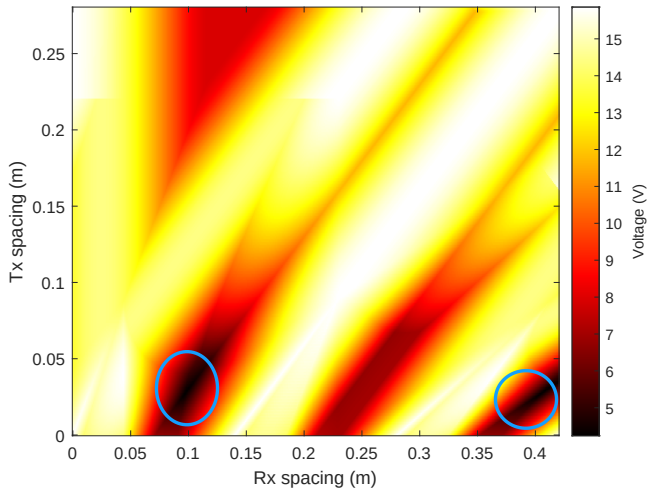

Figure 8.4: Heatmap showing the voltage fluctuation for different Tx- and Rx-coil spacings for the double Rx side system. The two blue circles indicate the optimal spacings.

The optimal coil placement could be at two different areas. Having the Tx-coil further apart is more

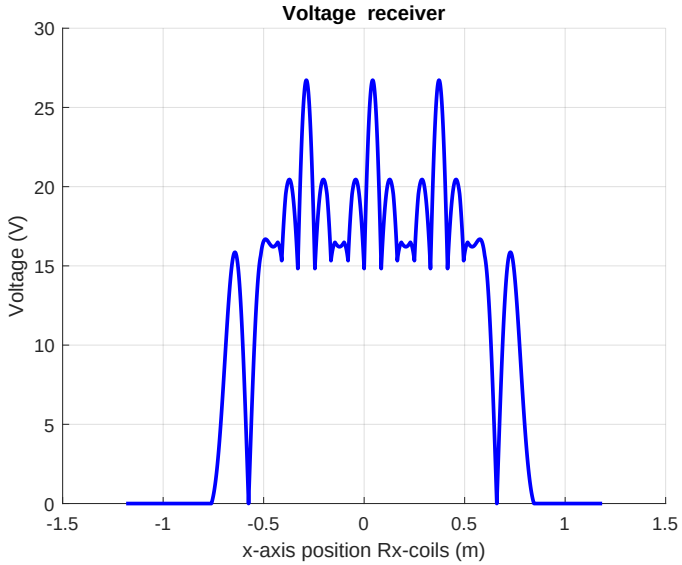

Figure 8.5: Output voltage with double Rx side system

beneficial than having the Rx-coils further apart. As a larger Tx-coil gap means less coils are needed, which makes the system cheaper. The optimal situation is when the Rx-coils have a spacing of 0.105 m in between them and the Tx-coils have a spacing of 0.05 m between each coil. The output voltage for these spacings is shown in Fig. 8.5. The figure shows that, in the area where both Rx-coils are over the Tx-coils, the voltage swings between a minimum of 14.8 V and a maximum of 26.6 V. The peak to peak voltage fluctuation is 44.4 %.

The original requirement was a maximum voltage fluctuation of 20 %, which means the system still does not uphold the requirement. Looking back, the requirement was too far of a reach for the scope of this project. In the future this requirement could be fulfilled by further optimizing the DIPT system, but for now the double Rx side system has only 44.4 % peak to peak voltage fluctuation compared to the 100 % of the originally proposed system. Therefore, it is recommended not to discard the double Rx side system. Testing still needs to be done to verify the results, nevertheless, the simulations promise an interesting basis for future work.

9

Discussion

The testing showed valuable insights for the other parts of the project. The first two tests were done to verify the accuracy of the COMSOL model and simulations. Three measurements are important for this. Firstly, the self inductance of the Tx-coil was measured to be 124.1 μH, whereas first COMSOL simulation gave 133.3 μH and the second COMSOL simulation gave 129.78 μH. The second COMSOL simulation was only 4.58 % off, which falls within the requirements set. Secondly, the first test showed a curve which deviated from the simulated data by being over 30 % lower. Thirdly, the second test showed that the first peak from the measurement curve was 9.01 % higher than the simulation. These three discrepancies raise questions about the accuracy of the measurements and simulations which were done.

More research should be done into the environmental factors that influence the mutual inductance measurement. One largely contributing factor was that the Tx-coils, and their ferrites, were glued on a plate. The advantage is that the measurements for the whole system can easily be repeated without having to measure the distance of the Tx-spacing. The problem is that one Tx-coil could not be separated from the rest for the first test. The first test showed a large deviation from the simulated results, while the second test with all coils deviated less from the simulations. The cause can likely be attributed to the interference from the other nearby Tx-coils and their ferrites. A new measurement should be performed in the future, separating the one Tx-coil from the track.

Furthermore, the COMSOL simulation does not take the connecting wires into account. As the Rx-coils move over the Tx-coils, the wires connecting the two tracks to the LCR meter can form a loop. While attention was payed to the wires during the measurements, such that they did not lay in between the Tx- and Rx-coils, it is possible that they might have formed a loop causing the data from the tests to be less accurate than the simulation.

In addition, the tests showed that the way the Rx-coils are connected can heavily influence the mutual inductance. The model that was designed whilst only looking into Rx coils in the series aiding configuration, without taking the opposing connection into account. After testing, the MATLAB script was modified to take this into account, and confirmed the hypotheses. The heatmaps do not yet include this data, which gave rise to the question if there exists a better solution with series opposing Rx-coils, than for series aiding connected Rx-coils.

For further work, it is recommended to use less data point from the COMSOL simulation. While extending the MATLAB to include a fourth Tx-coil was easily implementable as extendability was a system requirement. A fifth or sixth coil will be difficult due to lack of memory in MATLAB. The problem was already visible with a fourth coil when the spacing was very far apart, the data-set is too short and the data loops around. For future work this could be solved by cutting the amount of data points in half, while this will decrease the accuracy, the amount of data points will still be sufficient to model the mutual inductance. The mutual inductance curve in COMSOL has been simulated for a 1, 5, and 10 mm step-size and there is no significant difference between 1 or 5 mm.

For further optimization of the system, a deeper look into misalignment must be taken. While the topic was touched upon in Section 4.1, the simulation, model and testing did not include either y- or z-axis misalignment. In a dynamic EV charging system there might be hills or bumps in the road which could effect the z-misalignment. Moreover, self driving cars are still far away and human driver do not drive in a perfectly straight line. Research on this is already being done, with an example being the predictive model of the mutual inductance for different misalignment conditions [5].

Another point of future improvement would be to simulate the complete, multi-coil system on a computing cluster. This way, the mesh of the COMSOL model can be set to the finest, meaning that the simulation converges better. Next to that, having multiple Tx- and Rx-coils in COMSOL, means that some of the effects on the mutual inductance seen during testing, will be visible in the simulations.

10

Conclusion

For the system design, two major parts were discussed in this thesis: coil topology and the compensation circuit. Firstly, the coil topology is a combination of a bipolar and a rectangular coil. The higher misalignment tolerance of the bipolar coil is essential when implementing it as a DIPT EV charging system. Additionally, in further development the bipolar coil opened the opportunity for second receiver coil.

Secondly, to make the system more efficient, a compensation circuit was added. The compensation circuit will make the coils operate in resonance, so the power transfer is purely resistive. Two types were considered, an SS or DLCC circuit. The SS circuit performs better under aligned conditions, while the DLCC circuit performs better under misaligned conditions. The DLCC system was chosen because the Tx-current is independent of the mutual inductance which will help avoid high current stresses in misaligned conditions.

Next, the model was simulated in COMSOL to obtain data on the mutual inductance between the Tx- and Rx-coil. The accuracy of the final model was determined by comparing the self inductance of the measured Tx-coil 124.1 μH to that of the COMSOL model which was 133.3 μH. The simulation then ran a parametric sweep over a length of 0.6 m while the length of the bipolar coil is 0.28 m with a step size of 1 mm to obtain the data set that was used for the MATLAB script on the multiple coil system.

Subsequently, the data was put into an MATLAB script to determine the optimal Tx- and Rx-coil spacing. The data set from COMSOL is phase shifted and summed to represent three Tx-coils and two Rx-coils. The script used a nested for loop where the outer loop iterates the Rx-spacing, and the inner loop iterates the Tx-spacing, so the mutual inductance curve was determined for all spacing combinations. The script was later adjusted to take four Tx-coils into account, so the test result comparable to the simulation. Moreover, an explanation is given on how to adjust the script for series aiding or opposing connected Rx-coils.

Finally, the data was visualized into two heatmaps, one for the voltage fluctuation, and another for the average voltage. The ideal point is where the average voltage is high, while the voltage fluctuation is low. The spacing was determined to be 0.45 m for the Rx-coils and 0.1 m for the Tx-coils. The outcome gave a curve with zero crossings, which means the voltage fluctuation is depended on the average voltage.

The test verified part of the data from the COMSOL simulations and the MATLAB script. The first test, showed a similar curve for the mutual inductance versus the x-position between one Tx-coil and one Rx-coil. Testing showed that the vertical gap was actually 5.6 cm, implementing this in the COMSOL model improved the accuracy. However, the minimal and maximal mutual inductance revealed that the real values are more than 30 % lower in real life than the simulation. The second test showed strong indications that this error was due to interference from the other nearby Tx-coils.

The second test revealed that the coils were connected differently than the MATLAB simulations assumed. Two oddly sloped peaks in the curve made it apparent that the Rx coils were connected in

an opposing configuration in contrast to the assumption that they would be connected both with the windings in the same direction. To confirm this assumption the MATLAB script was rewritten and a fourth Tx-coil was added. Which resulted in more similar results. The third test showed that the output voltage has a curve similar to that of the mutual inductance. The highest peak is at 20.2 V and the lowest at 0 V, which exceeds the maximum voltage output ripple of 20 %.

Concluding that the originally proposed system fails to reduce the voltage fluctuations. An alternative system is proposed called the ”double phase Rx-coils”. The system connects the two Rx-coils to their own compensation circuit and rectifier, and connects their outputs in parallel. This way, zero voltage crossings can be avoided. The simulations show that the optimal situation is when the receiver coils have a spacing of 0.105 m in between them and the transmitter coils have a spacing of 0.05 m between each coil. With these spacings the peak to peak voltage fluctuations is 44.4 % from minimum to maximum, within the area of interest. While this does not uphold to the original requirements, the system offers a much more promising result than the originally proposed system.

A

Tables

This appendix contains tables with measured data, and properties used in COMSOL.

A.1. Circuit values

Table A.1: Measured values of the circuit components

Variables	Symbol	Unit	Value
Tx coil	L_{Tx}	μH	121.6
Rx coil	L_{Rx}	μH	111.2
Tx side compensation inductor	L_{f1}	μH	71.1
Rx side compensation inductor	L_{f2}	μH	47.2
Tx side parallel capacitor	C_{f1}	nF	48.0
Rx side parallel capacitor	C_{f2}	nF	74.9
Tx side series capacitor	C_{s1}	nF	51.6
Rx side series capacitor	C_{s2}	nF	54.5

A.2. Tables with material properties for COMSOL

Table A.2: The properties of air

Property	Variable	Expression	Unit
Coefficient of thermal expansion	alpha_iso	alpha_p(pA,T)	1/K
Mean molar mass	Mn	0.02897[kg/mol]	kg/mol
Bulk viscosity	muB	muB(T)	Pa·s
Relative permeability	mur_iso	1	1
Relative permittivity	epsilonr_iso	1	1
Dynamic viscosity	mu	eta(T)	Pa·s
Ratio of specific heats	gamma	1.4	1
Electrical conductivity	sigma_iso	10[S/m]	S/m
Heat capacity at constant pressure	Cp	Cp(T)	J/(kg·K)
Density	rho	rho(pA,T)	kg/m³
Thermal conductivity	k_iso	k(T)	W/(m·K)
Speed of sound	c	cs(T)	m/s

Table A.3: The properties of copper

Property	Variable	Expression	Unit
Relative permeability	mur_iso	1	1
Relative permittivity	epsilonr_iso	1	1
Electrical conductivity	sigma_iso	5.998e7[S/m]	S/m
Heat capacity at constant pressure	Cp	385[J/(kg*K)]	J/(kg·K)
Surface emissivity	epsilon_rad	0.5	1
Density	rho	8700[kg/m^3]	kg/m³
Thermal conductivity	k_iso	400[W/(m*K)]	W/(m·K)
Young's modulus	E	126e9[Pa]	Pa
Poisson's ratio	nu	0.34	1
Reference resistivity	rho0	1.72e-8[ohm*m]	Ω·m
Resistivity temperature coefficient	alpha	3.9e-3[1/K]	1/K
Reference temperature	Tref	273.15[K]	K

Table A.4: The properties of ferrite

Property	Variable	Expression	Unit
Relative permeability	mur_iso	4500	1
Electrical conductivity	sigma_iso	0.2 [S/m]	S/m
Relative permittivity	epsilonr_iso	1	1
Heat capacity at constant pressure	Cp	900 [J/(kg*K)]	J/(kg·K)
Thermal conductivity	k_iso	238 [W/(m*K)]	W/(m·K)
Coefficient of thermal expansion	alpha_iso	23e-6 [1/K]	1/K
Density	rho	2700 [kg/m^3]	kg/m³
Young's modulus	E	70e9 [Pa]	Pa
Poisson's ratio	nu	0.33	1
Murnaghan third-order elastic moduli	l	-2.5e11 [Pa]	N/m²
Murnaghan third-order elastic moduli	m	-3.3e11 [Pa]	N/m²

B

MATLAB

This appendix contains the MATLAB scripts used in this thesis.

B.1. Main

```
%%  Main


%parameters
f0      = 85000;    %switching frequency
w_out   = 0.14;     %outer radius of coil in m
I_tx    = 10;       %tx coil current

%import the mutual inductance data from COMSOL
run("import_script.m")
%and zero pad the dataset
run("data_padding.m")
%plot the data for COMSOL
%run("mutual_inductance_plot.m")

%NOTE: all of the distances and spacings in this script are in (m)!
n_tx_coils          = 3;    %number of tx-coils in the system
n_rx_coils          = 2;    %number of tx-coils in the system

tx_spacing_start    = w_out*2;      %start of tx-xoil spacing
tx_spacing_end      = w_out*6;      %end of tx-coil spacing
tx_spacing_step     = 0.001;        %step size of tx-coil spacing
tx_spacing          = (tx_spacing_start:tx_spacing_step:tx_spacing_end); %
    tx-coil spacing

rx_spacing_start    = w_out;    %start of rx-xoil spacing
rx_spacing_end      = w_out*6;      %end of rx-coil spacing
rx_spacing_step     = 0.001;        %step size of rx-coil spacing
rx_spacing          = (rx_spacing_start:rx_spacing_step:rx_spacing_end); %
    rx-coil spacing

dim_rx = length(rx_spacing);    %number of different Rx-coil spacings
dim_tx = length(tx_spacing);    %number of different Tx-coil spacings

%initialize multiple arrays
```

```
34 tx1_data = padded_data.mutual_inductance;                %first Rx-coil
       with first Tx-coil
35 tx2_data = zeros(data_length, dim_tx);                  %first Rx-coil with
        second Tx-coil
36 tx3_data = zeros(data_length, dim_tx);                  %first Rx-coil with
        third Tx-coil
37 rx1_data = zeros(data_length, dim_tx);                   %first Rx-coil
       with both Tx-coils
38 rx2_data = zeros(data_length, dim_rx, dim_tx);           %second Rx-coil
       with both Tx-coils
39 total_rx_data = zeros(data_length, dim_rx, dim_tx);      %both Rx-coils
       with both Tx-coils
40
41 %obtaining datasets for multiple Rx- and Tx-coils and their spacings
42 for n = 1:dim_rx
43     rx_coil_shift = int16(rx_spacing(n) / x_step_size);     %determine
           index of Rx-coil position
44     for k = 1:dim_tx
45         tx_coil_shift = int16(tx_spacing(k) / x_step_size);  %determine
               index of Tx-coil position
46
47         %step 1:
48         tx2_data(:,k) = circshift(tx1_data, tx_coil_shift);  %shift Tx1
               data to the right with Tx-spacing
49         tx3_data(:,k) = circshift(tx1_data, -tx_coil_shift); %shift Tx1
               data to the left with Tx-spacing
50
51         %step 2:
52         rx1_data(:, k) = tx1_data + tx2_data(:,k) + tx3_data(:,k);   %sum
               all Tx data to Rx1-coil
53
54         %step 3:
55         rx2_data(:, n, k) = circshift(rx1_data(:, k), rx_coil_shift);    %
               shift Rx1-data to Rx2-coil
56
57         %step 4:
58         total_rx_data(:, n, k) = rx1_data(:, k) + rx2_data(:, n, k);     %
               sum Rx-coils for total inductance data
59     end
60 end
61
62 %run("verification_plots.m")
63
64 %data for heatmaps
65 inductance_delta = zeros(dim_rx, dim_tx);   %initialize data
66 inductance_avg = zeros(dim_rx, dim_tx);
67 V_Rx_delta = zeros(dim_rx, dim_tx);
68 V_Rx_avg = zeros(dim_rx, dim_tx);
69 dx = 0.001;
70 s = zeros(dim_rx, dim_tx);
71 e = zeros(dim_rx, dim_tx);
72
73 %loop over all dataset combinations and trim their data
74 for i = 1:dim_rx
75     for j = 1:dim_tx
```

```
76          inductance_profile1 = rx1_data(:, j);   %mutual inductance of the
                first coil
77          k = 1;
78          while inductance_profile1(k) == 0   %find first point where mutual
                 inductance is non zero
79              k = k + 1;
80          end
81
82          l = data_length;
83          while inductance_profile1(l) == 0   %find last point where mutual
                inductance is non zero
84              l =l - 1;
85          end
86
87          inductance_profile2 = rx2_data(:, i, j); %mutual inductance of the
                 second coil
88          m = 1;
89          while inductance_profile2(m) == 0   %find first point where mutual
                 inductance is non zero
90              m = m + 1;
91          end
92
93          n = data_length;
94          while inductance_profile2(n) == 0   %find last point where mutual
                inductance is non zero
95              n=n-1;
96          end
97
98          if k >= m
99              s(i, j) = k;  %start point is l
100         else
101             s(i, j) = m;  %start point is k
102         end
103
104         if l <= n
105             e(i,j) = l;  %end point is m
106         else
107             e(i,j) = n;  %end point is n
108         end
109
110         inductance_profile = total_rx_data(:, i, j);    %total mutual
                inductance data for current coil spacings
111         trimmed_profile = inductance_profile(s(i,j):e(i,j));      %trim
                data to only include the points where rx1 and rx2 overlap
112
113         inductance_delta(i, j) = (max(trimmed_profile)-(trimmed_profile))
                /2);  %calculate the absolute difference over the current
                dataset
114         inductance_avg(i, j) = sum(inductance_profile*tx_spacing_step,1)/(
                x_data(e)-x_data(s));
115
116         V_Rx_delta(i, j) = inductance_delta(i, j) * (2*pi*f0*I_tx*10e-6);
117         V_Rx_avg(i, j) = inductance_avg(i, j) * (2*pi*f0*I_tx*10e-6);
118
119     end
120 end
```

B.2. Data Padding

```
%% Zeropadding COMSOL data set
padding     = 1000;  %number of zero's before and after data set

%padding of mutual inductance data
mutual_inductance_data = [zeros(padding, 1); mutualinductancesweep1.
    mutualInductanceRxtx1uH; zeros(padding, 1)];
data_length = length(mutual_inductance_data);   %length of the COMSOL
    dataset

%padding the x-axis data
x_step_size = mutualinductancesweep1.X_offsetm(2) -
    mutualinductancesweep1.X_offsetm(1);    %calculate x-axis step size
     from COMSOL data
x_start = mutualinductancesweep1.X_offsetm(1) - padding*x_step_size;
      %create new start value x-axis
x_data = (x_start: x_step_size : (x_start + (data_length - 1) *
    x_step_size))'; %create padded x-axis dataset

%create table with padded dataset
padded_data = table(x_data, mutual_inductance_data, 'Variablenames', {
    'x_data', 'mutual_inductance'});
```

B.3. Heatmaps

```
%%  Heatmaps


figure()
set(gca, 'FontName', 'Times New Roman', 'FontSize', 10)
set(gcf, 'Color', 'w')  % white background
imagesc(rx_spacing  - rx_spacing_start, tx_spacing - tx_spacing_start,
    inductance_delta');  %plot heatmap of average absolute mutual
    inductance delta
axis xy;
%title('\Delta Mutual Inductance across x\_data');
xlabel('Rx-coil spacing (m)');
ylabel('Tx-coil spacing (m)');
colorbar;
colormap('hot');
cb = colorbar;              % Add colorbar and get its handle
ylabel(cb, '\Delta mutual inductance across x-axis (uH)');   % Set label
    on the colorbar
exportgraphics(gcf, 'inductance_delta_heatmap.pdf', 'ContentType', 'vector
    ')

figure()
set(gca, 'FontName', 'Times New Roman', 'FontSize', 10)
set(gcf, 'Color', 'w')  % white background
imagesc(rx_spacing  - rx_spacing_start, tx_spacing - tx_spacing_start,
    V_Rx_delta');  %plot heatmap of average absolute mutual inductance
    delta
axis xy;
%title('\Delta output voltage across x\_data');
xlabel('Rx-coil spacing (m)');
ylabel('Tx-coil spacing (m)');
```

```
colorbar;
colormap('hot');
cb = colorbar;              % Add colorbar and get its handle
ylabel(cb, '\Delta output voltage across x-axis (V)');    % Set label on
    the colorbar
% Create ellipse
% Create ellipse
annotation('ellipse',...
    [0.487904761904762 0.207936507936508 0.129952380952381
       0.128571428571429]);

exportgraphics(gcf, 'voltage_delta_heatmap.pdf', 'ContentType', 'vector')

figure()
set(gca, 'FontName', 'Times New Roman', 'FontSize', 10)
set(gcf, 'Color', 'w')  % white background
imagesc(rx_spacing - rx_spacing_start, tx_spacing - tx_spacing_start,
    inductance_avg');  %plot heatmap of average absolute mutual inductance
    delta
axis xy;
%title('Avg. mutual inductance across x\_data');
xlabel('Rx-coil spacing (m)');
ylabel('Tx-coil spacing (m)');
colorbar;
colormap('hot');
cb = colorbar;              % Add colorbar and get its handle
ylabel(cb, 'average mutual inductance across x-axis (uH)');    % Set label
    on the colorbar
exportgraphics(gcf, 'inductance_average_heatmap.pdf', 'ContentType', '
    vector')

figure()
set(gca, 'FontName', 'Times New Roman', 'FontSize', 10)
set(gcf, 'Color', 'w')  % white background
imagesc(rx_spacing - rx_spacing_start, tx_spacing - tx_spacing_start,
    V_Rx_avg');  %plot heatmap of average absolute mutual inductance delta
axis xy;
%title('Avg. output voltage across x\_data');
xlabel('Rx-coil spacing (m)');
ylabel('Tx-coil spacing (m)');
colorbar;
colormap('hot');
cb = colorbar;              % Add colorbar and get its handle
ylabel(cb, 'average output voltage across x-axis (V)');    % Set label on
    the colorbar
% Create ellipse
annotation('ellipse',...
    [0.487904761904762 0.207936507936508 0.129952380952381
       0.128571428571429]);

exportgraphics(gcf, 'voltage_average_heatmap.pdf', 'ContentType', 'vector'
    )
```

B.4. Import script

```
    %% Set up the Import Options and import the data
```

```
    opts = delimitedTextImportOptions("NumVariables", 3);

    % Specify range and delimiter
    opts.DataLines = [6, Inf];
    opts.Delimiter = ",";

    % Specify column names and types
    opts.VariableNames = ["X_offsetm", "Var2", "mutualInductanceRxtx1uH"];
    opts.SelectedVariableNames = ["X_offsetm", "mutualInductanceRxtx1uH"];
    opts.VariableTypes = ["double", "string", "double"];

    % Specify file level properties
    opts.ExtraColumnsRule = "ignore";
    opts.EmptyLineRule = "read";

    % Specify variable properties
    opts = setvaropts(opts, "Var2", "WhitespaceRule", "preserve");
    opts = setvaropts(opts, "Var2", "EmptyFieldRule", "auto");

    % Import the data
    mutualinductancesweep1 = readtable("C:\Users\julie\Documents\TU\Y3\BAP
        \COMSOL_files\data\mutual_inductance_sweep_1.csv", opts);

    %% Clear temporary variables
    clear opts
```

B.5. Mutual inductance plot

```
%% Plot the mutual inductance versus relative Rx-coil position


figure()
set(gca, 'FontName', 'Times New Roman', 'FontSize', 10)
set(gcf, 'Color', 'w')  % white background
hold on
grid on
xlabel("x-axis position Rx-coil (m)")
ylabel("mutual inductance (uH)")
plot(mutualinductancesweep1.X_offsetm, mutualinductancesweep1.
    mutualInductanceRxtx1uH, 'blue')
exportgraphics(gcf, 'comsol_simulation.pdf', 'ContentType', 'vector')

figure()
set(gca, 'FontName', 'Times New Roman', 'FontSize', 10)
set(gcf, 'Color', 'w')  % white background
hold on
grid on
xlabel("x-axis position Rx-coil (m)")
ylabel("mutual inductance (uH)")
plot(padded_data.x_data, padded_data.mutual_inductance, 'blue')
exportgraphics(gcf, 'comsol_simulation_padded.pdf', 'ContentType', 'vector
    ')
```

B.6. Test 1 coil

```
% Define the test data for Position (x-axis) in mm
```

```
position = [
    2582; 2571;
    2563; 2552; 2545; 2534; 2528; 2522; 2515; 2506; 2498; 2488;
    2481; 2475; 2467; 2460; 2453; 2444; 2437; 2429; 2419; 2410;
    2400; 2392; 2385; 2380; 2372; 2364; 2357; 2350; 2342; 2333;
    2324; 2318; 2313; 2305; 2299; 2293; 2283; 2277; 2270; 2264;
    2257; 2251; 2245; 2237; 2231; 2225; 2216; 2211; 2205; 2199;
    2193; 2185; 2176
];
% Define the test data for measured total inductance in uH
mutualInductance = [
    179.9; 179.1;
    178.2; 176.7; 175.3; 172.9; 171.2; 170.6; 167.9; 164.6; 161.9; 158.7;
    156.4; 154.5; 152.5; 151.5; 150.8; 151.0; 151.7; 153.5; 157.0; 160.9;
    166.2; 170.1; 176.0; 178.7; 184.5; 188.6; 192.6; 198.0; 201.0; 204.4;
    206.7; 208.3; 208.5; 209.0; 208.9; 208.8; 207.3; 205.6; 203.6; 201.7;
    199.4; 197.8; 197.3; 193.6; 191.7; 189.5; 186.4; 185.9; 183.8; 183.0;
    182.9; 181.9; 181.3
];

mutualInductance = (mutualInductance - 180.16)/2;
offset = 2378;
x_position = position - offset;

% Convert COMSOL data from meters to mm
x1coilcomsol1 = mutualinductancesweep1.X_offsetm*1000;
M1coilcomsol1 = mutualinductancesweep1.mutualInductanceRxtx1uH;
%COMSOL 2 data for clarity
x1coilcomsol2 = x1coilcomsol;
M1coilcomsol2 = M1coilcomsol;

%import the mutual inductance data from COMSOL
run("import_script.m")

% Create combined plot
figure;
axis tight
set(gca, 'FontName', 'Times New Roman', 'FontSize', 10)
set(gcf, 'Color', 'w')  % white background
hold on;
plot(x1coilcomsol1, M1coilcomsol1, 'g', 'LineWidth', 2); % COMSOL 1 green
plot(x_position, mutualInductance, 'b', 'LineWidth', 2); % Test dataset in
    blue
plot(x1coilcomsol2, M1coilcomsol2, ':r', 'LineWidth', 2); % COMSOL 2 red
hold off;

% Add labels and legend
xlabel('x-axis position Rx-coils (mm)');
ylabel('mutual Inductance (uH)');
legend('COMSOL data 1', 'Test data', 'COMSOL data 2');
grid on;
exportgraphics(gcf, 'testing_and_comsol.pdf', 'ContentType', 'vector')
```

B.7. Testing plot

```
%%  Testing data and plotting
```

```
2
3
4  %testing data and parameters, these are all in mm!
5  zero_point = 1678;
6
7  rx_tot_inductance = 110.7;
8  tx_tot_inductance = 4*121;
9  tot_inductance = rx_tot_inductance + tx_tot_inductance;
10
11 position_offset = zero_point+30;
12 position_center = (position_data_1(1)-position_offset);
13
14 spacing_tx = 60;
15 spacing_rx = 0.274;
16 w_out = 140;
17
18 figure()
19 set(gca, 'FontName', 'Times New Roman', 'FontSize', 10)
20 set(gcf, 'Color', 'w')  % white background
21 hold on
22 grid on
23 xlabel("x-axis position Rx-coils (mm)")
24 ylabel("mutual Inductance (uH)")
25
26 plot(position_data_1-position_offset, inductance_1-tot_inductance, 'blue',
       'LineWidth',2)
27 plot(position_data_2-position_offset, inductance_2-tot_inductance, ':red',
       'LineWidth',2)
28 xline(position_center+w_out)
29 xline(position_center-w_out)
30 xline(position_center+w_out+spacing_tx)
31 xline(position_center+3*w_out+spacing_tx)
32 xline(position_center-w_out-spacing_tx)
33 xline(position_center-3*w_out-spacing_tx)
34
35 legend("Measurement 1", "Measurement 2")
36 exportgraphics(gcf, 'testing_result.pdf', 'ContentType', 'vector')
```

B.8. Verification plots

```
1  %%  Verification
2
3
4  %spacings to plot
5  plot_rx_spacing = 0.45;  %plotted rx spacing in m
6  plot_tx_spacing = 0.1;  %plotted rx spacing in m
7
8  plot_rx_index = int16(plot_rx_spacing/rx_spacing_step) + 1; %calculate rx
       index for plot
9  plot_tx_index = int16(plot_tx_spacing/tx_spacing_step) + 1; %calculate tx
       index for plot
10
11 %x-axis
12 x_axis = (0 : data_length - 1) * x_step_size;   %create and x-axis
13 x_center = (x_axis(end)-x_axis(1))/2;
14
```

```
%data to plot
%orignal:
tx1_rx1 = tx1_data;
%step 1:
tx2_rx1 = tx2_data(:, plot_tx_index);
tx3_rx1 = tx3_data(:, plot_tx_index);
%step 2:
tx_rx1 = rx1_data(:, plot_tx_index);
%step 3:
tx_rx2 = rx2_data(:, plot_rx_index, plot_tx_index);
%step 4:
tx_rx_total = total_rx_data(:, plot_rx_index, plot_tx_index);
%trimed profile:
trimmed_tx_rx_total = total_rx_data(s(plot_rx_index, plot_tx_index):e(
    plot_rx_index, plot_tx_index), plot_rx_index, plot_tx_index);
trimmed_x_axis = x_axis(s(plot_rx_index, plot_tx_index):e(plot_rx_index,
    plot_tx_index));

%plots of the different steps
%step 1 & 2:
figure()
set(gca, 'FontName', 'Times New Roman', 'FontSize', 10)
set(gcf, 'Color', 'w')  % white background
hold on
grid on
%title(”Mutual inductance profile for step 1 & 2”)
xlabel(”x-axis position Rx-coils (m)”)
ylabel(”mutual inductance (uH)”)

plot(x_axis, tx1_rx1, 'blue', 'LineWidth',2)
plot(x_axis, tx2_rx1, 'cyan', 'LineWidth',2)
plot(x_axis, tx3_rx1, 'green', 'LineWidth',2)
plot(x_axis, tx_rx1, ':red', 'LineWidth',2)

xline(x_center+w_out)
xline(x_center-w_out)
xline(x_center+w_out+plot_tx_spacing)
xline(x_center-w_out-plot_tx_spacing)
xline(x_center+3*w_out+plot_tx_spacing)
xline(x_center-3*w_out-plot_tx_spacing)

legend(”Tx_1”, ”Tx_2”, ”Tx_3”, ”Tx_{total}”)
exportgraphics(gcf, 'step_1_2.pdf', 'ContentType', 'vector')

%step 3 & 4:
figure()
set(gca, 'FontName', 'Times New Roman', 'FontSize', 10)
set(gcf, 'Color', 'w')  % white background
hold on
grid on
%title('Mutual Inductance Profile for step 3 & 4');
xlabel(”x-axis position Rx-coils (m)”);
ylabel(”mutual inductance (uH)”);

plot(x_axis, tx_rx1, 'blue', 'LineWidth',2)
plot(x_axis, tx_rx2, 'cyan', 'LineWidth',2)
```

```
plot(x_axis, tx_rx_total, ':red', 'LineWidth',2)

xline(x_center+w_out)
xline(x_center-w_out)
xline(x_center+w_out+plot_tx_spacing)
xline(x_center-w_out-plot_tx_spacing)
xline(x_center+3*w_out+plot_tx_spacing)
xline(x_center-3*w_out-plot_tx_spacing)

legend("Rx_1", "Rx_2", "Rx_{total}")
exportgraphics(gcf, 'step_3_4.pdf', 'ContentType', 'vector')

%result
figure()
set(gca, 'FontName', 'Times New Roman', 'FontSize', 10)
set(gcf, 'Color', 'w')  % white background
hold on
grid on
%title('Total Mutual Inductance Profile');
xlabel("x-axis position Rx-coils (m)");
ylabel("mutual inductance (uH)");

fill([x_axis(s(plot_rx_index, plot_tx_index)) x_axis(e(plot_rx_index,
   plot_tx_index)) x_axis(e(plot_rx_index, plot_tx_index)) x_axis(s(
   plot_rx_index, plot_tx_index))], [-40 -40 40 40], [1 0 0], 'FaceAlpha',
    0.1, 'EdgeColor', 'none');  % light red
plot(x_axis, tx_rx_total, 'blue', 'LineWidth',2)

xline(x_center+w_out)
xline(x_center-w_out)
xline(x_center+w_out+plot_tx_spacing)
xline(x_center-w_out-plot_tx_spacing)
xline(x_center+3*w_out+plot_tx_spacing)
xline(x_center-3*w_out-plot_tx_spacing)
xline(x_axis(s(plot_rx_index, plot_tx_index)), '--r')
xline(x_axis(e(plot_rx_index, plot_tx_index)), '--r')

legend("area of interest", "Rx_{total}")
exportgraphics(gcf, 'total_result.pdf', 'ContentType', 'vector')

%trimmed result
figure()
set(gca, 'FontName', 'Times New Roman', 'FontSize', 10)
set(gcf, 'Color', 'w')  % white background
hold on
grid on
%title('Trimmed Total Mutual Inductance Profile');
xlabel("x-axis position Rx-coils (m)");
ylabel("mutual inductance (uH)");

plot(trimmed_x_axis, trimmed_tx_rx_total, 'blue', 'LineWidth',2)

legend("trimmed Rx_{total}")
exportgraphics(gcf, 'trimmed_total_result.pdf', 'ContentType', 'vector')
```

B.9. Main 2

```
%%  Main


%parameters
f0      = 85000;    %switching frequency
w_out   = 0.14;     %outer radius of coil in m
I_tx    = 10;       %tx coil current

%import the mutual inductance data from COMSOL
%run("import_script.m")
%and zero pad the dataset
run("data_padding.m")
%plot the data for COMSOL
%run("mutual_inductance_plot.m")

%NOTE: all of the distances and spacings in this script are in (m)!
n_tx_coils          = 3;    %number of tx-coils in the system
n_rx_coils          = 2;    %number of tx-coils in the system

tx_spacing_start    = w_out*2;      %start of tx-xoil spacing
tx_spacing_end      = w_out*6;      %end of tx-coil spacing
tx_spacing_step     = 0.001;        %step size of tx-coil spacing
tx_spacing          = (tx_spacing_start:tx_spacing_step:tx_spacing_end); %
    tx-coil spacing

rx_spacing_start    = w_out;    %start of rx-xoil spacing
rx_spacing_end      = w_out*6;      %end of rx-coil spacing
rx_spacing_step     = 0.001;        %step size of rx-coil spacing
rx_spacing          = (rx_spacing_start:rx_spacing_step:rx_spacing_end); %
    rx-coil spacing

dim_rx = length(rx_spacing);    %number of different Rx-coil spacings
dim_tx = length(tx_spacing);    %number of different Tx-coil spacings

%initialize multiple arrays
tx1_data = padded_data.mutual_inductance;               %first Rx-coil
    with first Tx-coil
tx2_data = zeros(data_length, dim_tx);                %first Rx-coil with
     second Tx-coil
tx3_data = zeros(data_length, dim_tx);                %first Rx-coil with
     third Tx-coil
tx4_data = zeros(data_length, dim_tx);                %first Rx-coil with
     third Tx-coil
rx1_data = zeros(data_length, dim_tx);                %first Rx-coil
    with both Tx-coils
rx2_data = zeros(data_length, dim_rx, dim_tx);          %second Rx-coil
    with both Tx-coils
total_rx_data = zeros(data_length, dim_rx, dim_tx);     %both Rx-coils
    with both Tx-coils

%obtaining datasets for multiple Rx- and Tx-coils and their spacings
for n = 1:dim_rx
    rx_coil_shift = int16(rx_spacing(n) / x_step_size);     %determine
        index of Rx-coil position
    for k = 1:dim_tx
```

```
46        tx_coil_shift = int16(tx_spacing(k) / x_step_size);  %determine
              index of Tx-coil position
47
48        %step 1:
49        tx2_data(:,k) = circshift(tx1_data, tx_coil_shift);  %shift Tx1
              data to the right with Tx-spacing
50        tx3_data(:,k) = circshift(tx1_data, -tx_coil_shift); %shift Tx1
              data to the left with Tx-spacing
51        tx4_data(:,k) = circshift(tx1_data, 2*tx_coil_shift); %shift Tx1
              data to the left with Tx-spacing
52        %step 2:
53        rx1_data(:, k) = tx1_data + tx2_data(:,k) + tx3_data(:,k)+ tx4_data
              (:,k);   %sum all Tx data to Rx1-coil
54
55        %step 3:
56        rx2_data(:, n, k) = circshift(-rx1_data(:, k), -rx_coil_shift);
              %shift Rx1-data to Rx2-coil
57
58        %step 4:
59        total_rx_data(:, n, k) = -(rx1_data(:, k) + rx2_data(:, n, k));
                %sum Rx-coils for total inductance data
60    end
61 end
62
63 run("verification_plots.m")
64
65 %data for heatmaps
66 inductance_delta = zeros(dim_rx, dim_tx);   %initialize data
67 inductance_avg = zeros(dim_rx, dim_tx);
68 V_Rx_delta = zeros(dim_rx, dim_tx);
69 V_Rx_avg = zeros(dim_rx, dim_tx);
70 dx = 0.001;
71
72 %loop over all dataset combinations and trim their data
73 for i = 1:dim_rx
74     for j = 1:dim_tx
75         inductance_profile1 = rx1_data(:, j);   %mutual inductance of the
              first coil
76         k = 1;
77         while inductance_profile1(k) == 0   %find first point where mutual
               inductance is non zero
78             k = k + 1;
79         end
80
81         l = data_length;
82         while inductance_profile1(l) == 0   %find last point where mutual
              inductance is non zero
83             l =l - 1;
84         end
85
86         inductance_profile2 = rx2_data(:, i, j); %mutual inductance of the
               second coil
87         m = 1;
88         while inductance_profile2(m) == 0   %find first point where mutual
               inductance is non zero
89             m = m + 1;
```

```
90          end
91
92          n = data_length;
93          while inductance_profile2(n) == 0   %find last point where mutual
                inductance is non zero
94              n=n-1;
95          end
96
97          if k >= m
98              s = k;  %start point is l
99          else
100             s = m;  %start point is k
101         end
102
103         if l <= n
104             e = l;  %end point is m
105         else
106             e = n;  %end point is n
107         end
108
109         inductance_profile = total_rx_data(:, i, j);    %total mutual
                inductance data for current coil spacings
110         trimmed_profile = inductance_profile(s:e);      %trim data to only
                 include the points where rx1 and rx2 overlap
111
112         inductance_delta(i, j) = (max(trimmed_profile)-(trimmed_profile))
                /2);  %calculate the absolute difference over the current
                dataset
113         inductance_avg(i, j) = sum(inductance_profile*tx_spacing_step,1)/(
                x_data(e)-x_data(s));
114
115         V_Rx_delta(i, j) = inductance_delta(i, j) * (2*pi*f0*I_tx*10e-6);
116         V_Rx_avg(i, j) = inductance_avg(i, j) * (2*pi*f0*I_tx*10e-6);
117
118     end
119 end
```

B.10. Verification plots 2

```
1  %%  Verification
2
3
4  %spacings to plot
5  plot_rx_spacing = 0.274;  %plotted rx spacing in m
6  plot_tx_spacing = 0.06;  %plotted rx spacing in m
7
8  plot_rx_index = int16(plot_rx_spacing/rx_spacing_step) + 1; %calculate rx
       index for plot
9  plot_tx_index = int16(plot_tx_spacing/tx_spacing_step) + 1; %calculate tx
       index for plot
10
11 %x-axis
12 x_axis = (0 : data_length - 1) * x_step_size;   %create and x-axis
13 x_center = (x_axis(end)-x_axis(1))/2;
14
15 %data to plot
```

```
%orignal:
tx1_rx1 = tx1_data;
%step 1:
tx2_rx1 = tx2_data(:, plot_tx_index);
tx3_rx1 = tx3_data(:, plot_tx_index);
tx4_rx1 = tx4_data(:, plot_tx_index);
%step 2:
tx_rx1 = rx1_data(:, plot_tx_index);
%step 3:
tx_rx2 = rx2_data(:, plot_rx_index, plot_tx_index);
%step 4:
tx_rx_total = total_rx_data(:, plot_rx_index, plot_tx_index);
%trimed profile:

%plots of the different steps
%step 1 & 2:
figure()
set(gca, 'FontName', 'Times New Roman', 'FontSize', 10)
set(gcf, 'Color', 'w')  % white background
hold on
grid on
%title(”Mutual inductance profile for step 1 & 2”)
xlabel(”x-axis position Rx-coils (m)”)
ylabel(”mutual inductance (uH)”)

plot(x_axis, tx1_rx1, 'blue', 'LineWidth',2)
plot(x_axis, tx2_rx1, 'cyan', 'LineWidth',2)
plot(x_axis, tx3_rx1, 'green', 'LineWidth',2)
plot(x_axis, tx4_rx1, 'magenta', 'LineWidth',2)
plot(x_axis, tx_rx1, ':red', 'LineWidth',2)

xline(x_center+w_out)
xline(x_center-w_out)
xline(x_center+w_out+plot_tx_spacing)
xline(x_center-w_out-plot_tx_spacing)
xline(x_center+3*w_out+plot_tx_spacing)
xline(x_center-3*w_out-plot_tx_spacing)
xline(x_center+w_out+plot_tx_spacing+2*w_out+plot_tx_spacing)
xline(x_center+w_out+plot_tx_spacing+2*w_out+plot_tx_spacing+2*w_out)

legend(”Tx_1”, ”Tx_2”, ”Tx_3”, ”Tx_4”, ”Tx_{total}”)
exportgraphics(gcf, '4_step_1_2.pdf', 'ContentType', 'vector')


%step 3 & 4:
figure()
set(gca, 'FontName', 'Times New Roman', 'FontSize', 10)
set(gcf, 'Color', 'w')  % white background
hold on
grid on
%title('Mutual Inductance Profile for step 3 & 4');
xlabel(”x-axis position Rx-coils (m)”);
ylabel(”mutual inductance (uH)”);

plot(x_axis, tx_rx1, 'blue', 'LineWidth',2)
plot(x_axis, tx_rx2, 'cyan', 'LineWidth',2)
```

```
plot(x_axis, tx_rx_total, ':red', 'LineWidth',2)

xline(x_center+w_out)
xline(x_center-w_out)
xline(x_center+w_out+plot_tx_spacing)
xline(x_center-w_out-plot_tx_spacing)
xline(x_center+3*w_out+plot_tx_spacing)
xline(x_center-3*w_out-plot_tx_spacing)
xline(x_center+w_out+plot_tx_spacing+2*w_out+plot_tx_spacing)
xline(x_center+w_out+plot_tx_spacing+2*w_out+plot_tx_spacing+2*w_out)

legend(”Rx_1”, ”Rx_2”, ”Rx_{total}”)
exportgraphics(gcf, '4_step_3_4.pdf', 'ContentType', 'vector')

%result
figure()
set(gca, 'FontName', 'Times New Roman', 'FontSize', 10)
set(gcf, 'Color', 'w')  % white background
hold on
grid on
%title('Total Mutual Inductance Profile');
xlabel(”x-axis position Rx-coils (m)”);
ylabel(”mutual inductance (uH)”);

plot(x_axis, tx_rx_total, 'blue', 'LineWidth',2)

xline(x_center+w_out)
xline(x_center-w_out)
xline(x_center+w_out+plot_tx_spacing)
xline(x_center-w_out-plot_tx_spacing)
xline(x_center+3*w_out+plot_tx_spacing)
xline(x_center-3*w_out-plot_tx_spacing)
xline(x_center+w_out+plot_tx_spacing+2*w_out+plot_tx_spacing)
xline(x_center+w_out+plot_tx_spacing+2*w_out+plot_tx_spacing+2*w_out)

legend(”Rx_{total}”)
exportgraphics(gcf, 'total_result_opposing.pdf', 'ContentType', 'vector')
```

B.11. Main script for double Rx

```
%%  Main


%parameters
f0      = 0.085000;    %switching frequency
w_out   = 0.14;     %outer radius of coil in m
I_tx    = 1.32;       %tx coil current

%import the mutual inductance data from COMSOL
run(”import_script.m”)
%and zero pad the dataset
run(”data_padding.m”)
%plot the data for COMSOL
%run(”mutual_inductance_plot.m”)

%NOTE: all of the distances and spacings in this script are in (m)!
```

```
17 n_tx_coils          = 3;    %number of tx-coils in the system
18 n_rx_coils          = 2;    %number of tx-coils in the system
19
20 tx_spacing_start    = w_out*2;      %start of tx-xoil spacing
21 tx_spacing_end      = w_out*4;      %end of tx-coil spacing
22 tx_spacing_step     = 0.001;        %step size of tx-coil spacing
23 tx_spacing          = (tx_spacing_start:tx_spacing_step:tx_spacing_end); %
       tx-coil spacing
24
25 rx_spacing_start    = w_out;    %start of rx-xoil spacing
26 rx_spacing_end      = w_out*4;      %end of rx-coil spacing
27 rx_spacing_step     = 0.001;        %step size of rx-coil spacing
28 rx_spacing          = (rx_spacing_start:rx_spacing_step:rx_spacing_end); %
       rx-coil spacing
29
30 dim_rx = length(rx_spacing);    %number of different Rx-coil spacings
31 dim_tx = length(tx_spacing);    %number of different Tx-coil spacings
32
33 %initialize multiple arrays
34 tx1_data = padded_data.mutual_inductance;               %first Rx-coil
       with first Tx-coil
35 tx2_data = zeros(data_length, dim_tx);                 %first Rx-coil with
        second Tx-coil
36 tx3_data = zeros(data_length, dim_tx);                 %first Rx-coil with
        third Tx-coil
37 tx4_data = zeros(data_length, dim_tx);                 %first Rx-coil with
        third Tx-coil
38 rx1_data = zeros(data_length, dim_tx);                  %first Rx-coil
       with both Tx-coils
39 rx2_data = zeros(data_length, dim_rx, dim_tx);          %second Rx-coil
       with both Tx-coils
40 v_rx1_data = zeros(data_length, dim_tx);                  %first Rx-coil
       with both Tx-coils
41 v_rx2_data = zeros(data_length, dim_rx, dim_tx);          %second Rx-coil
       with both Tx-coils
42 total_rx_data = zeros(data_length, dim_rx, dim_tx);     %both Rx-coils
       with both Tx-coils
43 v_rx_data = zeros(data_length, dim_rx, dim_tx);     %both Rx-coils with
       both Tx-coils
44
45 %obtaining datasets for multiple Rx- and Tx-coils and their spacings
46 for n = 1:dim_rx
47     rx_coil_shift = int16(rx_spacing(n) / x_step_size);     %determine
          index of Rx-coil position
48     for k = 1:dim_tx
49        tx_coil_shift = int16(tx_spacing(k) / x_step_size);  %determine
             index of Tx-coil position
50
51        %step 1:
52        tx2_data(:,k) = circshift(tx1_data, tx_coil_shift);  %shift Tx1
             data to the right with Tx-spacing
53        tx3_data(:,k) = circshift(tx1_data, -tx_coil_shift); %shift Tx1
             data to the left with Tx-spacing
54        tx4_data(:,k) = circshift(tx1_data, 2*tx_coil_shift); %shift Tx1
             data to the left with Tx-spacing
55        %step 2:
```

```
56          rx1_data(:, k) = tx1_data + tx2_data(:,k) + tx3_data(:,k)+tx4_data
                (:,k);   %sum all Tx data to Rx1-coil
57
58          %step 3:
59          rx2_data(:, n, k) = circshift(-rx1_data(:, k), -rx_coil_shift);
                %shift Rx1-data to Rx2-coil
60
61          %step 4:
62          total_rx_data(:, n, k) = (rx1_data(:, k) + rx2_data(:, n, k));
                %sum Rx-coils for total inductance data
63          v_rx1_data(:, k)=abs(rx1_data(:, k)*2*pi*f0*I_tx);
64          v_rx2_data(:, n, k)=abs(rx2_data(:, n, k)*2*pi*f0*I_tx);
65          v_rx_data(:, n, k) = (v_rx1_data(:, k) + v_rx2_data(:, n, k));
66      end
67  end
68
69
70  run("verification_plots_v.m")
71  %%
72  %data for heatmaps
73  V_delta = zeros(dim_rx, dim_tx);   %initialize data
74  V_avg = zeros(dim_rx, dim_tx);
75  V_Rx_delta = zeros(dim_rx, dim_tx);
76  V_Rx_avg = zeros(dim_rx, dim_tx);
77  dx = 0.001;
78
79  %loop over all dataset combinations and trim their data
80  for i = 1:dim_rx
81      for j = 1:dim_tx
82          inductance_profile1 = rx1_data(:, j);   %mutual inductance of the
                first coil
83          k = 1;
84          while inductance_profile1(k) == 0   %find first point where mutual
                inductance is non zero
85              k = k + 1;
86          end
87
88          l = data_length;
89          while inductance_profile1(l) == 0   %find last point where mutual
                inductance is non zero
90              l =l - 1;
91          end
92
93          inductance_profile2 = rx2_data(:, i, j); %mutual inductance of the
                second coil
94          m = 1;
95          while inductance_profile2(m) == 0   %find first point where mutual
                inductance is non zero
96              m = m + 1;
97          end
98
99          n = data_length;
100         while inductance_profile2(n) == 0   %find last point where mutual
                inductance is non zero
101             n=n-1;
102         end
```

```
103
104         if k >= m
105             s = k;  %start point is l
106         else
107             s = m;  %start point is k
108         end
109
110         if l <= n
111             e = l;  %end point is m
112         else
113             e = n;  %end point is n
114         end
115
116         v_profile = v_rx_data(:, i, j);    %total mutual inductance data
                for current coil spacings
117         trimmed_profile = v_profile(s:e);      %trim data to only include
                the points where rx1 and rx2 overlap
118
119         V_delta(i, j) = (max(trimmed_profile)-min(trimmed_profile))/2;  %
                calculate the absolute difference over the current dataset
120         V_avg(i, j) = (sum(trimmed_profile*tx_spacing_step,1))/(x_data(e)-
                x_data(s));   %calculate the absolute difference the result
                over the current the current dataset
121         %inductance_avg(i,j) = mean(abs(trimmed_profile));
122     end
123 end
124
125 run("heatmaps.m")
126 %run("test_1coil.m")
```

B.12. Voltage plots double Rx system

```
1  %spacings to plot
2  plot_rx_spacing = 0.105;  %plotted rx spacing in m
3  plot_tx_spacing = 0.05;  %plotted rx spacing in m
4
5  plot_rx_index = int16(plot_rx_spacing/rx_spacing_step) + 1; %calculate rx
       index for plot
6  plot_tx_index = int16(plot_tx_spacing/tx_spacing_step) + 1; %calculate tx
       index for plot
7
8  %x-axis
9  x_axis =  ((0 : data_length - 1) - (data_length - 1) / 2) * x_step_size;
        %create and x-axis
10 x_center = 0;
11
12 %data to plot
13 %orignal:
14 tx1_rx1 = v_rx_data(:, plot_rx_index, plot_tx_index);
15 %step 1:
16 tx2_rx1 = v_rx1_data(:, plot_tx_index);
17 tx3_rx1 = v_rx2_data(:, plot_rx_index, plot_tx_index);
18
19 %plots of the different steps
20 %step 1 & 2:
21 figure()
```

```
22 hold on
23 grid on
24 title(”Voltage  receiver”)
25 xlabel(”x-axis position Rx-coils (m)”)
26 ylabel(”Voltage (V)”)
27 plot(x_axis, tx1_rx1, 'blue', 'LineWidth',2)
28 %plot(x_axis, tx2_rx1, 'cyan', 'LineWidth',2)
29 %plot(x_axis, tx3_rx1, ':red', 'LineWidth',2)
```

Bibliography

[1] Bogdan Adamczyk, Nick Koeller, and Megan Healy. *Estimating the parasitics of passive circuit components*. Apr. 2024. URL: https://incompliancemag.com/estimating-the-parasitics-of-passive-circuit-components/.

[2] Kunwar Aditya and Sheldon S. Williamson. "A Review of Optimal Conditions for Achieving Maximum Power Output and Maximum Efficiency for a Series–Series Resonant Inductive Link". In: *IEEE Transactions on Transportation Electrification* 3.2 (2017), pp. 303–311. DOI: 10.1109/TTE.2016.2582559.

[3] Soumya Bandyopadhyay et al. "Comparison of Optimized Chargepads for Wireless EV Charging Application". In: *2019 10th International Conference on Power Electronics and ECCE Asia (ICPE 2019 - ECCE Asia)*. 2019, pp. 1–8. DOI: 10.23919/ICPE2019-ECCEAsia42246.2019.8796904.

[4] R. Bosshard. "Multi-Objective Optimization of Inductive Power Transfer Systems for EV Charging". PhD thesis. ETH Zürich, 2015. DOI: 10.3929/ethz-a-010664107. URL: https://www.research-collection.ethz.ch/handle/20.500.11850/117204.

[5] G. Di Capua et al. "Analysis of Dynamic Wireless Power Transfer Systems Based on Behavioral Modeling of Mutual Inductance". In: *Sustainability* 13.5 (2021), p. 2556. DOI: 10.3390/su13052556. URL: https://www.mdpi.com/2071-1050/13/5/2556.

[6] Su Y. Choi et al. "Advances in Wireless Power Transfer Systems for Roadway-Powered Electric Vehicles". In: *IEEE Journal of Emerging and Selected Topics in Power Electronics* 3.1 (2015), pp. 18–36. DOI: 10.1109/JESTPE.2014.2343674.

[7] V. Cirimele. "Design and Integration of a Dynamic IPT System for Automotive Applications". Master's thesis. Politecnico di Torino, 2017.

[8] Hemant Kumar Dashora et al. "Analysis and design of DD coupler for dynamic wireless charging of electric vehicles". In: *Journal of Electromagnetic Waves and Applications* 32.2 (2018), pp. 170–189. DOI: 10.1080/09205071.2017.1373036. URL: https://doi.org/10.1080/09205071.2017.1373036.

[9] M. Feliziani et al. *Introduction to Wireless Power Transfer for E-Mobility*. Elsevier eBooks, Jan. 2024, pp. 1–24. DOI: 10.1016/b978-0-323-99523-8.00004-7. URL: https://doi.org/10.1016/b978-0-323-99523-8.00004-7.

[10] Nathan Wezi van Himbergen and Stefan Kort. *Controller*. 2025.

[11] S. Kisseleff, I. F. Akyildiz, and W. Gerstacker. "Beamforming for Magnetic Induction Based Wireless Power Transfer Systems with Multiple Receivers". In: *Proc. IEEE Global Communications Conf. (GLOBECOM)*. 2014, pp. 1–7. DOI: 10.1109/glocom.2014.7417006. URL: https://doi.org/10.1109/glocom.2014.7417006.

[12] Tsong-Shing Lee et al. "Design of Misalignment-Insensitive Inductive Power Transfer via Interoperable Coil Module and Dynamic Power Control". In: *IEEE Transactions on Power Electronics* 35.9 (2020), pp. 9024–9033. DOI: 10.1109/TPEL.2020.2972035. URL: https://doi.org/10.1109/TPEL.2020.2972035.

[13] Jorg Leijten. "Cijfer van de dag: 20 miljoen autos". In: *NRC* (May 2025). URL: https://www.nrc.nl/nieuws/2025/05/14/cijfer-van-de-dag-20-miljoen-autos-a4893167.

[14] J. Li, F. Wang, and Y. He. "Electric Vehicle Routing Problem with Battery Swapping Considering Energy Consumption and Carbon Emissions". In: *Sustainability* 12.24 (2020), p. 10537. DOI: 10.3390/su122410537. URL: https://www.mdpi.com/2071-1050/12/24/10537.

[15] K. Li et al. “Application of Wireless Energy Transmission Technology in Electric Vehicles”. In: *Renewable and Sustainable Energy Reviews* 184 (2023), p. 113569. DOI: 10.1016/j.rser.2023.113569. URL: https://www.sciencedirect.com/science/article/pii/S1364032123004264.

[16] Chunting Chris Mi et al. “Modern Advances in Wireless Power Transfer Systems for Roadway Powered Electric Vehicles”. In: *IEEE Transactions on Industrial Electronics* 63.10 (2016), pp. 6533–6545. DOI: 10.1109/TIE.2016.2574993.

[17] A. A. S. Mohamed et al. “An Overview of Dynamic Inductive Charging for Electric Vehicles”. In: *Energies* 15.15 (2022), p. 5613. DOI: 10.3390/en15155613. URL: https://doi.org/10.3390/en15155613.

[18] C. Panchal, S. Stegen, and J. Lu. “Review of Static and Dynamic Wireless Electric Vehicle Charging System”. In: *Eng. Sci. Technol. Int. J.* 21.5 (June 2018), pp. 922–937. DOI: 10.1016/j.jestch.2018.06.015. URL: https://doi.org/10.1016/j.jestch.2018.06.015.

[19] *Questions and answers LCR meter*. URL: https://www.mrclab.com/questions-and-answers-lcr-meter.

[20] W. Shi. “Dynamic Wireless Charging of Electric Vehicles”. In: *resolver.tudelft.nl* (2023). DOI: 10.4233/c469a4fa-92bc-4ddf-9790-bd9f7a248815. URL: https://doi.org/10.4233/c469a4fa-92bc-4ddf-9790-bd9f7a248815.

[21] Jaegue Shin et al. “Design and Implementation of Shaped Magnetic-Resonance-Based Wireless Power Transfer System for Roadway-Powered Moving Electric Vehicles”. In: *IEEE Transactions on Industrial Electronics* 61.3 (2014), pp. 1179–1192. DOI: 10.1109/TIE.2013.2258294.

[22] M. Simonazzi, L. Sandrolini, and A. Mariscotti. “Receiver–Coil Location Detection in a Dynamic Wireless Power Transfer System for Electric Vehicle Charging”. In: *Sensors* 22.6 (Mar. 2022), p. 2317. DOI: 10.3390/s22062317. URL: https://doi.org/10.3390/s22062317.

[23] L. Van Der Sluis and P. Schavemaker. *Electrical Power System Essentials*. 2nd ed. Wiley, 2017.

[24] Jesse Treurniet and Owen Wattenbergh. *Converter*. 2025.

[25] Fawwaz Tayssir Ulaby and Umberto Ravaioli. *Maxwell’s Equations for Time-Varying Fields*. Prentice Hall, Jan. 2015.

[26] Chengliang Wang and Honghua Wang. “Research on output power stability control method of EV-DWPT system”. In: *Electrical Engineering* 104.3 (Aug. 2021), pp. 1247–1254. DOI: 10.1007/s00202-021-01382-7. URL: https://doi.org/10.1007/s00202-021-01382-7.

[27] Zhiyuan Wang et al. “A Novel Magnetic Coupling Mechanism for Dynamic Wireless Charging System for Electric Vehicles”. In: *IEEE Transactions on Vehicular Technology* 67.1 (2018), pp. 124–133. DOI: 10.1109/TVT.2017.2776348.

[28] C. Yang. “Running Battery Electric Vehicles with Extended Range: Coupling Cost and Energy Analysis”. In: *Appl. Energy* 306 (Nov. 2021), p. 118116. DOI: 10.1016/j.apenergy.2021.118116. URL: https://doi.org/10.1016/j.apenergy.2021.118116.

[29] Adeel Zaheer et al. “Investigation of Multiple Decoupled Coil Primary Pad Topologies in Lumped IPT Systems for Interoperable Electric Vehicle Charging”. In: *IEEE Transactions on Power Electronics* 30.4 (2015), pp. 1937–1955. DOI: 10.1109/TPEL.2014.2329693.

[30] Xueyi Zhang, Changhui Quan, and Zhongqi Li. “Mutual Inductance Calculation of Circular Coils for an Arbitrary Position With Electromagnetic Shielding in Wireless Power Transfer Systems”. In: *IEEE Transactions on Transportation Electrification* 7.3 (2021), pp. 1196–1204. DOI: 10.1109/TTE.2021.3054762.

[31] Q. Zhu et al. “Applying LCC Compensation Network to Dynamic Wireless EV Charging System”. In: *IEEE Trans. Ind. Electron.* 63.10 (2016), pp. 6557–6567. DOI: 10.1109/TIE.2016.2529561.